

**Zeitschrift:** IABSE reports of the working commissions = Rapports des commissions de travail AIPC = IVBH Berichte der Arbeitskommissionen

**Band:** 11 (1971)

**Rubrik:** Prepared discussion

#### **Nutzungsbedingungen**

Die ETH-Bibliothek ist die Anbieterin der digitalisierten Zeitschriften auf E-Periodica. Sie besitzt keine Urheberrechte an den Zeitschriften und ist nicht verantwortlich für deren Inhalte. Die Rechte liegen in der Regel bei den Herausgebern beziehungsweise den externen Rechteinhabern. Das Veröffentlichen von Bildern in Print- und Online-Publikationen sowie auf Social Media-Kanälen oder Webseiten ist nur mit vorheriger Genehmigung der Rechteinhaber erlaubt. [Mehr erfahren](#)

#### **Conditions d'utilisation**

L'ETH Library est le fournisseur des revues numérisées. Elle ne détient aucun droit d'auteur sur les revues et n'est pas responsable de leur contenu. En règle générale, les droits sont détenus par les éditeurs ou les détenteurs de droits externes. La reproduction d'images dans des publications imprimées ou en ligne ainsi que sur des canaux de médias sociaux ou des sites web n'est autorisée qu'avec l'accord préalable des détenteurs des droits. [En savoir plus](#)

#### **Terms of use**

The ETH Library is the provider of the digitised journals. It does not own any copyrights to the journals and is not responsible for their content. The rights usually lie with the publishers or the external rights holders. Publishing images in print and online publications, as well as on social media channels or websites, is only permitted with the prior consent of the rights holders. [Find out more](#)

**Download PDF:** 30.01.2026

**ETH-Bibliothek Zürich, E-Periodica, <https://www.e-periodica.ch>**

### III

## DISCUSSION PRÉPARÉE / VORBEREITETE DISKUSSION / PREPARED DISCUSSION

### Discussion of the Report by Professor P. Dubas:

"Essais sur le comportement post-critique de poutres en caisson raidies"

The Conventional Design of Box Girders is unsafe and must be the — at least partial — Cause of the Recent Collapse of Three Large Box Girders Bridges

### Discussion du rapport du Prof. P. Dubas:

"Essais sur le comportement post-critique de poutres en caisson raidies"

### Diskussion über den Bericht von Prof. P. Dubas:

"Essais sur le comportement post-critique de poutres en caisson raidies"

R. MAQUOI

Aspirant du Fonds National  
de la Recherche Scientifique  
Belgique

CH. MASSONNET

Professeur  
à l'Université de Liège

### 1. INTRODUCTION.

The striking result obtained by professor DUBAS in the test of a box girder described in his report, namely a mean collapse stress less than the critical stress derived from linear buckling theory (see sec.8), has crystallized some grave doubts we had since several years about the safety of the conventional design of box girders. We hold the opinion that, if the safety factor  $s$  of about 1.35 against the critical stress of linear buckling theory, adopted in several countries, was justified in the case of the web of a plate girder, because of the stabilizing effect of a postcritical diagonal tension field, the use of the same coefficient for designing the compressed flange of a box girder was totally unjustified, because the stabilizing effect of membrane stresses is, in this case, much less than in the first one.

It may be appropriate to recall here that the senior author has repeatedly insisted [1, 2] on the fact that theoretically strictly rigid stiffeners, (that means stiffeners of relative rigidity  $\gamma^*$  given by linear buckling theory) were never rigid in practice and gave girders with a low safety, barely able to reach 0.95 to 1 times the yield point in the flanges at collapse. To ensure stiffeners remaining effectively straight up to collapse, it was necessary to adopt values  $\gamma = m\gamma^*$  with  $m$  varying between 3 and 8. The effect of this increase in the rigidity of the stiffeners was to increase the strength by about 25 per cent. This experimental fact has been confirmed recently by OWEN, ROCKEY and SKALOUD [3].

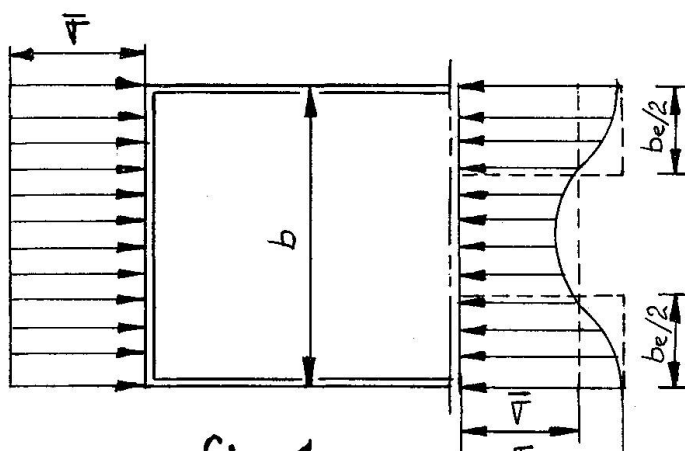
The senior author was therefore convinced that box girders with flanges stiffened by  $\gamma^*$  stiffeners had a particularly low effective safety against collapse.

Now, the spectacular accidents which have struck, during last year, three large steel box girder bridges, namely the bridge over the Danube in Vienna on 6 November 1969, the bridge of Milford Haven in Great Britain on 2 June 1970 and the bridge over the lower Yarra in Melbourne (Australia) on 15 October 1970, have reinforced these doubts about the validity of the linear buckling theory.

It seems demonstrated that, in the case of the Danube bridge at least, the collapse occurred for mean compression stresses barely equal to the critical stress of the linear theory. This would mean that, in this case, at least, no reserve of postcritical strength existed.

One of the purposes of present report is to show theoretically that this is actually the case (see section 6).

The compressed flange of a box girder subjected to bending is not, like the web of a plate girder, strengthened by a rigid frame constituted of the flanges of the girder and the adjacent transverse stiffeners. On the contrary, the most plausible assumption regarding the boundary conditions of this flange is simple support with complete freedom of the plate edges to move and deform in the plane of the plate. The instability phenomenon of such plates is nearer to that of the compressed column than to that of a plate girder web subjected to shear. In particular, unavoidable imperfections such as buckles due to the welding sequence should exert a strong deteriorating influence. (see sec. 6). In otherwords, the transverse distribution of compressive stresses is far from remaining uniform up to collapse. Effectively, as is clearly shown in fig. 8 of DUBAS report, the stress diagram shows a central pocket of increasing magnitude. The stresses in the middle are lagging behind the edge stresses (Fig. 1). When these latter reach the yield point, the capacity of the box girder is practically exhausted (see sec. 4) and the box girder collapses.



-fig. 1-

buckling.

Summarizing, the aim of present report is to prove that the reduction of the mean stress due to buckling, enhanced by imperfections, may upset the gain due to non linear membrane stresses, so that finally the mean collapse stress  $\sigma$  of the imperfect flange may become even less than the critical stress of the perfect flange according to linear buckling theory (see sec. 6). There is therefore an urgent need to push forward the theoretical and experimental investigation and, pending these researches, to increase notably the safety factors of box girders against plate

In waiting for these investigations, we have tried to draw the best information from the few papers at our disposal (sec. 2 to 4).

## 2. SOME CONSIDERATIONS ABOUT THE COLEAPSE OF THREE BOX GIRDER BRIDGES.

As told above, we imagine that the fundamental inadequacy of linear buckling theory as applied to the design of large box girders may have played a role in the recent collapse of three large box girder bridges. As we have been able to collect detailed information only in the case of the bridge at Vienna, we shall restrict ourselves to the study of this case.

The circumstances of the collapse of the Danube bridge near Vienna seem rather clear [4, 5]. According to professor SATTLER's paper [5], the three experts took following position regarding the causes of the accident:

1. The calculation of erection stresses was made for a uniformly distributed

loading. The actual distribution of the dead weight differs from this assumption and gave at one of the damaged places more unfavourable conditions, so that in reality at this place larger stresses have existed and therefore smaller-buckling and collapse safeties.

2. The temperature effect in the steel structure on the day of the bridge closing had a value that was not to be expected from the responsible personnel from the temperature observations of the preceding days. This fact diminished the safety factor against collapse.
3. Besides, there existed constructive as well as unavoidable imperfections (which diminished the safety factor). Taking these imperfections into account is not necessary, according to the specifications, but is covered by the required safety factors. In present case, where the safety against collapse was already diminished by circumstances 1 and 2 above, the imperfections have played a non negligible role as partial cause of the accident
4. The collapse of the entire lower flange of the box girder at a place precipitated the collapse of the whole cross section. The redistribution of internal forces which ensued necessarily explain all other damages as consequences of the first one.

Professor SATTLER has been very kind to send us the detailed report he established as expert for the bridge collapse. According to this report: The safety factor adopted during erection was :

- 1.25. against yielding
- 1.25 against buckling calculated by linear theory.

The steel used was St 44, with a yield point of  $\sigma_y = 2900 \text{ Kg/cm}^2$ .

At the section where the first buckling damage must have occurred, the lower compressed flange had a breadth of 7600 mm, a thickness of 10 mm ( $b/t = 760$ ) and was stiffened by 12 flat stiffeners 160 x 12 mm.

According to professor SATTLER's report, the relative rigidity of these stiffeners was chosen strictly to obtain a buckling coefficient  $k$  of the whole panel equal to that of a subpanel, namely  $k = 4 \times (12 + 1)^2 = 676$ .

In other words, the relative rigidity of these stiffeners was equal to  $\gamma^*$

The ideal buckling stress found in the calculations was  $\sigma_{cr}^{id} = 2,235 \text{ Kg/cm}^2$  and the reduced buckling stress taking account of plasticity,  $\sigma_{cr}$  was, according to the Austrian Specifications,  $\sigma_{cr} = 2,213 \text{ Kg/cm}^2$ .

According to professor SATTLER's calculations, due to the circumstances indicated above, the mean stress in the compressed flange must have reached at the time of collapse, the value

$$\bar{\sigma}_{max} = 2,224 \text{ Kg/cm}^2.$$

SATTLER considers that the condition  $\sigma_{max} = \sigma_{cr}$  is the explanation of the collapse.

We completely agree with this explanation, especially because we shall show in section 6 that collapse can occur even for values of the mean stress  $\bar{\sigma}$  less than  $\sigma_{cr}$ .

## 3. FOUNDATIONS OF THE NON LINEAR THEORY OF BUCKLING OF COMPRESSED PLATES.

The non linear theory of buckling of plates has been developed by von Karman and is represented by following coupled fourth order equations

$$\frac{D}{t} \nabla^2 \nabla^2 w = \frac{\partial^2 \phi}{\partial x^2} \frac{\partial^2 w}{\partial y^2} + \frac{\partial^2 \phi}{\partial y^2} \frac{\partial^2 w}{\partial x^2} - 2 \frac{\partial^2 \phi}{\partial x \partial y} \frac{\partial^2 w}{\partial x \partial y} \quad (1)$$

$$\nabla^2 \nabla^2 \phi = E \left[ \left( \frac{\partial^2 w}{\partial x \partial y} \right)^2 - \frac{\partial^2 w}{\partial x^2} \frac{\partial^2 w}{\partial y^2} \right] \quad (2)$$

where:  $w$  is the transverse displacement of the plate,

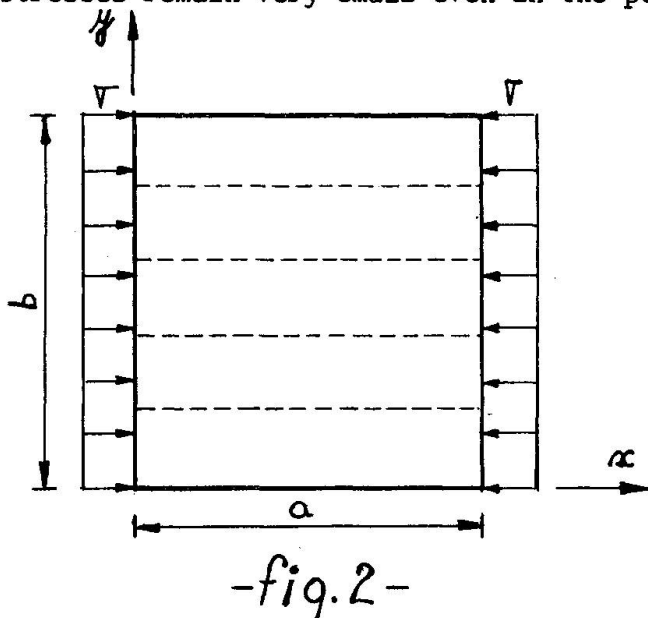
$$D = \frac{Et^3}{12(1-\nu^2)} \text{ its flexural rigidity ,}$$

$t$  the thickness

$\nu$  Poisson's ratio,

$\phi$  Airy's stress function.

The stiffened plates constituting the compressed flanges of box girders are supported at their edges in such a way that these edges can move freely in the plate's plane. If the box girder is subjected to pure bending, as in professor DUBAS experiments, there are no shear stresses along the lateral edges before buckling, and it seems reasonable to admit that these shear stresses remain very small even in the postbuckling range. Therefore, the



boundary conditions of the stiffened compressed plate ( $a \times b$ ) of fig. 2 may be taken as :  
for  $x = 0$  and  $x = a$  :

$$w = \frac{\partial^2 w}{\partial x^2} + \nu \frac{\partial^2 w}{\partial y^2} = 0 \quad (3)$$

$$\frac{\partial^2 \phi}{\partial y^2} = \sigma, \quad \frac{\partial^2 \phi}{\partial x \partial y} = 0$$

for  $y = 0$  and  $y = b$  :

$$w = \frac{\partial^2 w}{\partial y^2} + \nu \frac{\partial^2 w}{\partial x^2} = 0 \quad (4)$$

$$\frac{\partial^2 \phi}{\partial x^2} = 0, \quad \frac{\partial^2 \phi}{\partial x \partial y} = 0$$

Starting from equations (1) and (2) with boundary condition (3), (4), SKALOUD and NOVOTNY, in two papers ([7], [8]), have brought a very important contribution to the solution of the problem, for the case of one median longitudinal stiffener or of two stiffeners placed at the thirds of the width. Later on, they have sketched the solution of the same problem when account is taken of the effect of initial deformation or stresses ([9], [10]). The solution is based on Rayleigh-Ritz energy method. As the authors have not taken account of the potential energy corresponding to the compression of the stiffeners, the results obtained do not depend on the relative area of the stiffeners, and are valid only for  $\delta = \frac{A}{bt} = 0$ .

On the other hand, numerical results are given only for the square plate

( $\alpha \equiv a/b = 1$ ); however, their paper contains the cubic equations which would enable to develop the calculations for other values of  $\alpha$

#### 4. COLLAPSE CRITERION ADOPTED.

SKALOUD and NOVOTNY admit that the strength of the plate is exhausted when the maximum membrane stress  $\sigma_{xm}$  which occurs along the unloaded edges reaches the yield point  $\sigma_y$  of the steel used. In the case where the stiffeners remain rigid up to collapse, the membrane stresses  $\sigma_{xm}^r$  in the plate at the location of the stiffeners reach also  $\sigma_y$ .

The validity of above collapse criterion has been extensively discussed by SKALOUD in other papers (see e.g. [11]). It neglects two circumstances which have opposite effects: the bending stresses in the plate and the plastic redistribution after the yield point has been reached. We admit that these effects cancel each other and therefore the validity of SKALOUD's criterion.

#### 5. CHARTS FOR THE SQUARE PLATE.

From the diagrams obtained by SKALOUD and NOVOTNY for a square plate with one or two equidistant stiffeners, we have constructed the charts of figures 3 and 4. Figures 3a and b apply to the plate with one stiffener, figures 4a and b to the plate with two stiffeners. We have only considered values of the stiffener's relative rigidity  $\gamma = \frac{EI}{BD}$  for which  $\gamma > \gamma^*$ .

##### First problem.

Given a square steel plate whose dimensions  $a = b$ ,  $t$ , are known, it is asked to determine the rigidity  $\gamma_p^*$  required from the stiffener(s), in order that this (these) remain rigid up to collapse, as well as the value of the collapse mean stress  $\bar{\sigma}$ .

The solution is immediate by figures 3a and 4a.  $\bar{\sigma}$  and  $\gamma_p^*$  depend only on the thinness  $b/t$  of the plate and their values are obtained at the intersection of the corresponding curves with the horizontal of the ordinate  $b/t$ .

A vertical drawn from the  $\gamma_p^*$  value to the curve of factors  $m = \frac{\gamma}{\gamma^*}$ , gives the multiplier of value of  $\gamma^*$ , which itself is known in function of  $\alpha$  and of the relative area  $\delta$  (see note at the bottom of next page)

By the relation

$$m \gamma^* = 10,92 \frac{I_r}{b t^3},$$

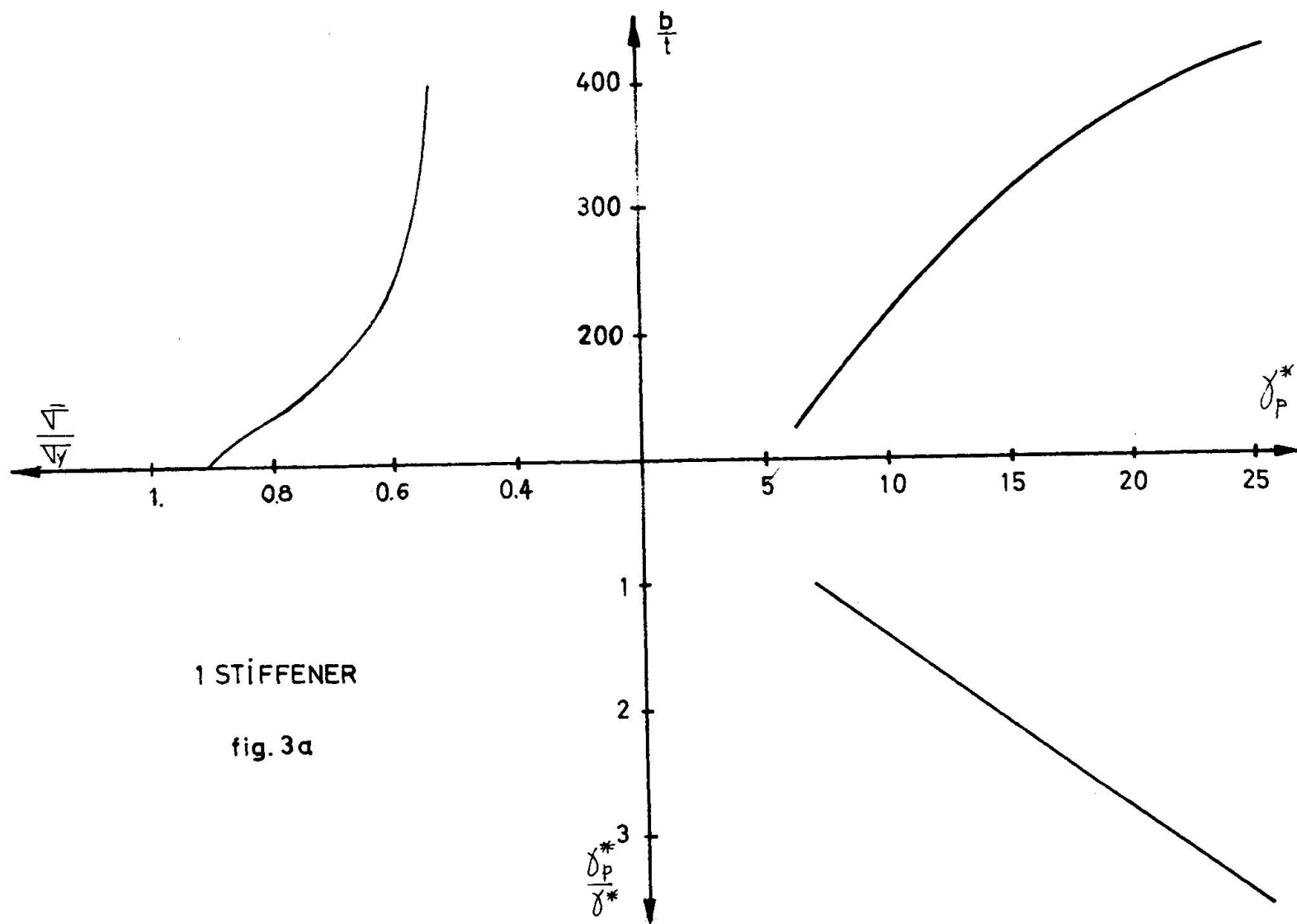
the moment of inertia of the stiffener(s) required becomes

$$I_r = \frac{m \gamma^* b t^3}{10,92}$$

##### Example:

$a = b = 200 \text{ cm}$ ,  $t = 0,8 \text{ cm}$ . One stiffener

Figure 4a gives for  $b/t = 200/0.8 = 250$



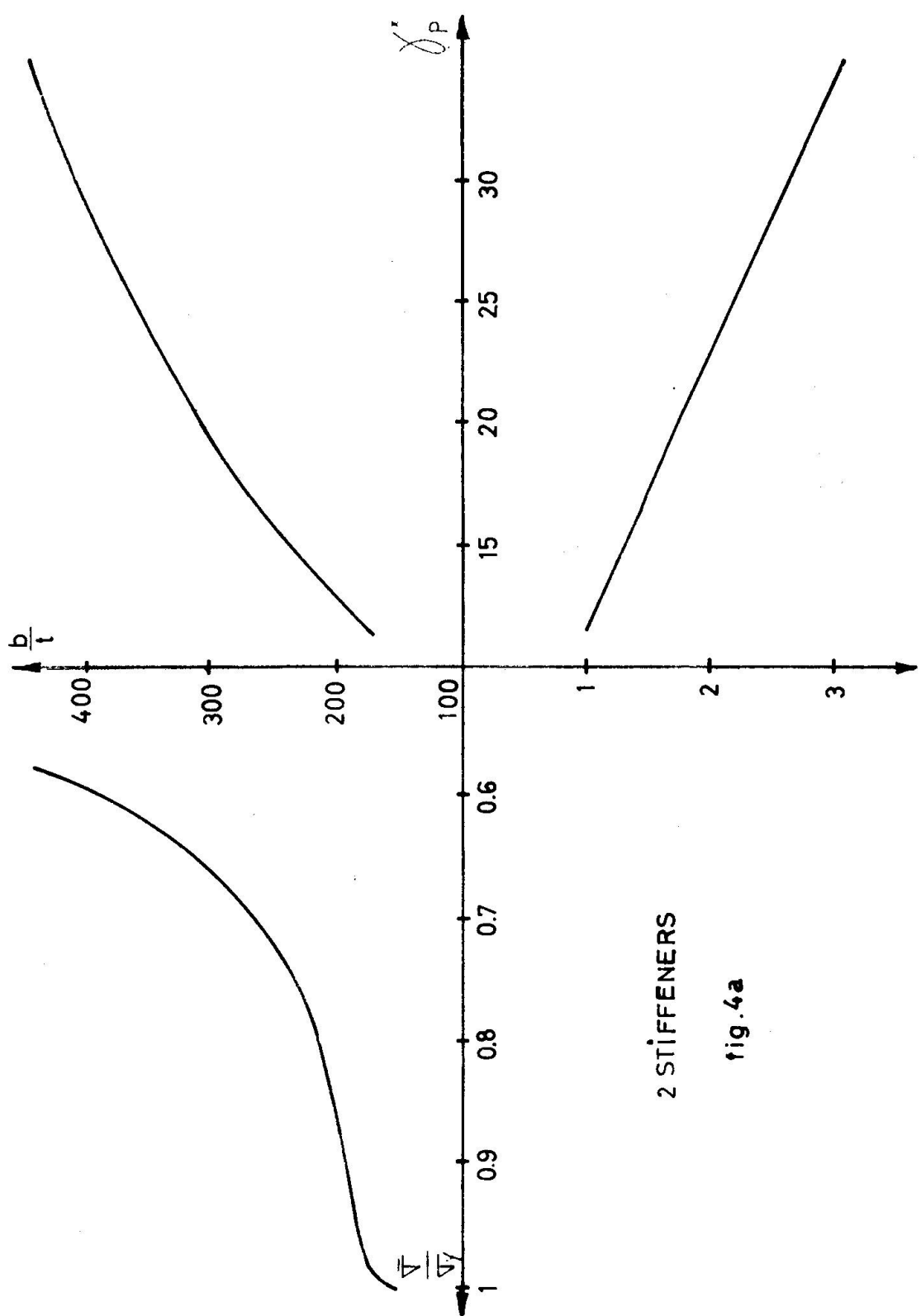
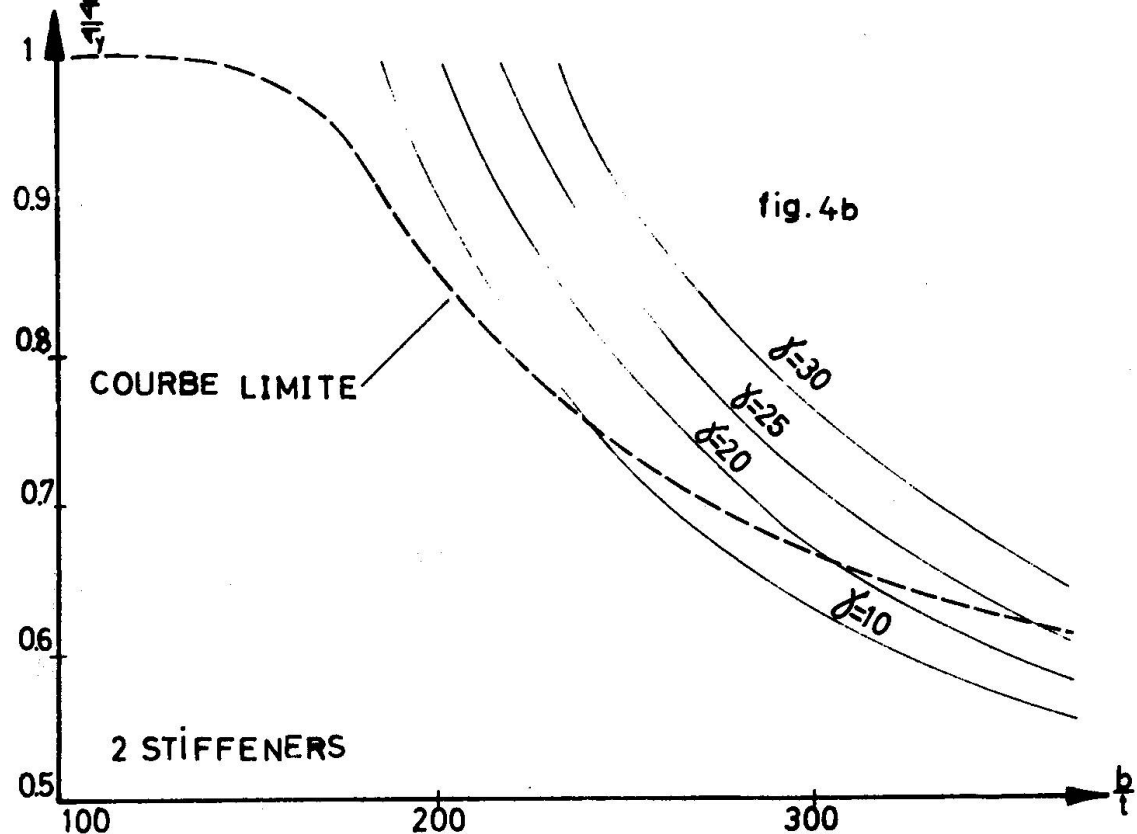
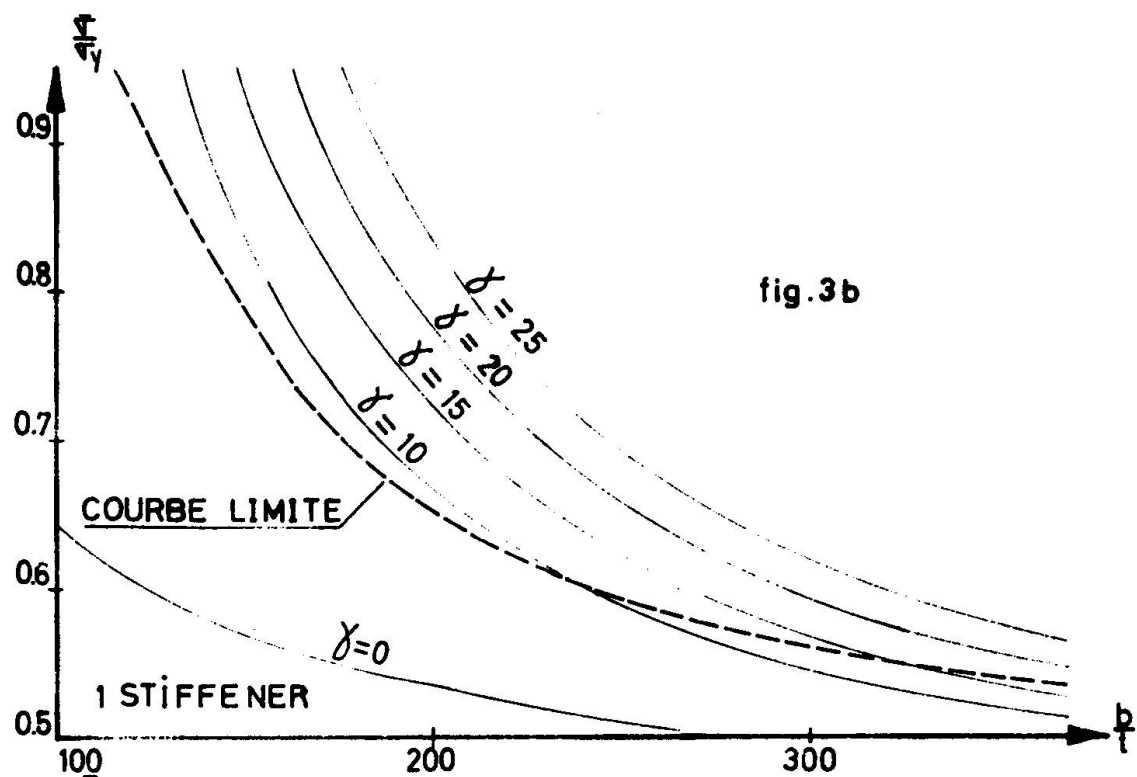


fig. 4a



$$\frac{\bar{\sigma}}{\sigma_y} = 0.59, \text{ whence } \bar{\sigma} = 1416 \text{ Kg/cm}^2.$$

$$\gamma^* = 11.6. \text{ whence } m = 1.65.$$

The moment of inertia of the stiffener must at least be  $I_r = 109 \text{ cm}^4$ .

Second problem.

Given a square plate whose dimensions  $a = b$ ,  $t$  are known, stiffened by one (two) stiffener(s) of given relative rigidity, it is asked to determine his ultimate strength.

The solution is immediate by figures 3b and 4b, established for a yield point  $\sigma = 2400 \text{ Kg/cm}^2$ . These figures give the value of  $\bar{\sigma}/\sigma_y$  as a function of the thinness  $b/t$  of the plate.

The various curves correspond to definite values of  $\gamma$ .

Example:  $a = b = 400 \text{ cm}$  ;  $t = 1 \text{ cm}$  ;  $I_r = 549.5 \text{ cm}^4$ .

First, the relative rigidity

$$\gamma = \frac{10.92 \times 549.5}{400 \times 1} = 15$$

is calculated. Then, from figures 3b or 4b, one reads :

a) for one stiffener :  $\frac{\bar{\sigma}}{\sigma_y} = 0.515$

b) for two stiffeners :  $\frac{\bar{\sigma}}{\sigma_y} = 0.530$

(\*)

$\delta$  being the ratio  $\frac{\text{area of the stiffener's cross section}}{\text{area of the cross section of the plate}} = \frac{A_r}{bD}$ ,

one has:

$$\text{one stiffener: } \alpha \leq \sqrt{8(1+2\delta)-1} : \gamma^* = \frac{\alpha^2}{2} [16(1+2\delta)-2] - \frac{\alpha^4}{2} + \frac{1+2\delta}{2}$$

$$\alpha \geq \sqrt{8(1+2\delta)-1} : \gamma^* = \frac{1}{2} [8(1+2\delta)-1]^2 + \frac{1+2\delta}{2}$$

two stiffeners :

$$\alpha \leq \sqrt{18(1+3\delta)-1} : \gamma^* = \frac{\alpha^2}{3} [36(1+3\delta)-2] - \frac{\alpha^4}{3} + \frac{1+3\delta}{3}$$

$$\alpha \geq \sqrt{18(1+3\delta)-1} : \gamma^* = \frac{1}{3} [18(1+3\delta)-1]^2 + \frac{1+3\delta}{3}.$$

## 6. EFFECT OF AN INITIAL DEFORMATION.

SKALOUD and NOVOTNY have studied in [9] the effect of an initial deformation of a stiffened plate on its ultimate strength for the case of one median stiffener. They have established for this case and for various values of the relative rigidity  $\gamma$  of the stiffener charts giving  $\bar{\sigma}/\sigma_y$  (for  $\sigma_y = 2400 \text{ Kg/cm}^2$ ) as function of the relative thinness  $b/t$  of the plate. The curves are labelled in terms of  $f_o/t$ , where  $f_o$  is the initial deflection in the middle of the panel and  $t$  the plate thickness. The shape of the initial deformation is

$$w_o = f_o \sin \frac{\pi x}{a} \sin \frac{\pi y}{b}.$$

and the boundary conditions are the same as previously.

The collapse criterion is the same as that discussed in section 4.

The loss in ultimate strength is especially marked for small values of the thinness  $b/t$  and becomes negligible for a certain value of  $b/t$  which is the smallest for stiffeners with the largest values of the relative rigidity.

Figures 5 and 6 reproduce the charts of SKALOUD and NOVOTNY for the values  $\gamma = 10$  and  $20$  of the relative rigidity, and for  $f_o/t = 0, 1, 2$ . The curve corresponding to  $f_o/t = 2$  has been obtained from the curves  $f_o/t=0$  and  $f_o/t = 1$  by assuming the  $\bar{\sigma}/\sigma_y$  varies linearly with  $f_o/t$  for  $b/t$  fixed, which is approximately correct.

In test N° 1 of professor DUBAS, (see his fig. 11, p. 14), one has an initial deflection  $f_o = 4.8 \text{ mm}$  for a thickness  $t = 3.3 \text{ mm}$ . The corresponding ratio  $f_o/t = 1.46$ . As it concerns a laboratory test where the specimens are fabricated with especial care, it is logical to admit that, in an actual bridge, the ratio  $f_o/t$  may reach 2.

Above theoretical results are limited to the case of a single stiffener. Pending new researches, we have supposed that they can be extended to a plate with two longitudinal stiffeners under following assumptions:

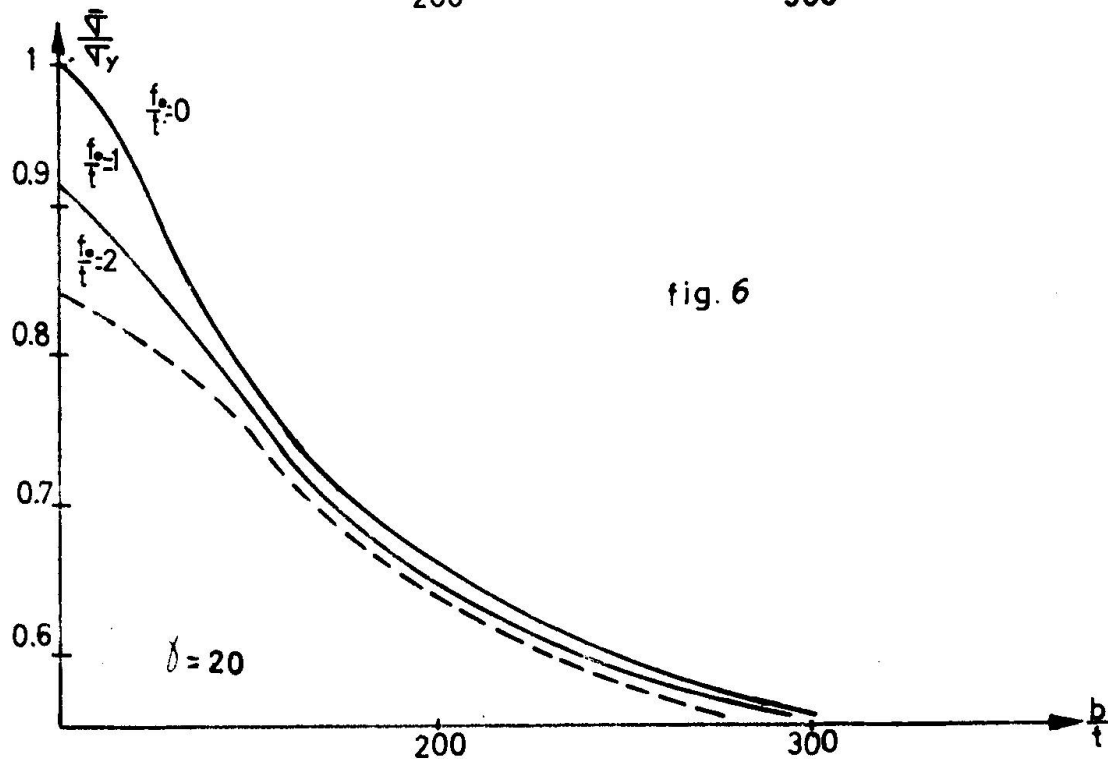
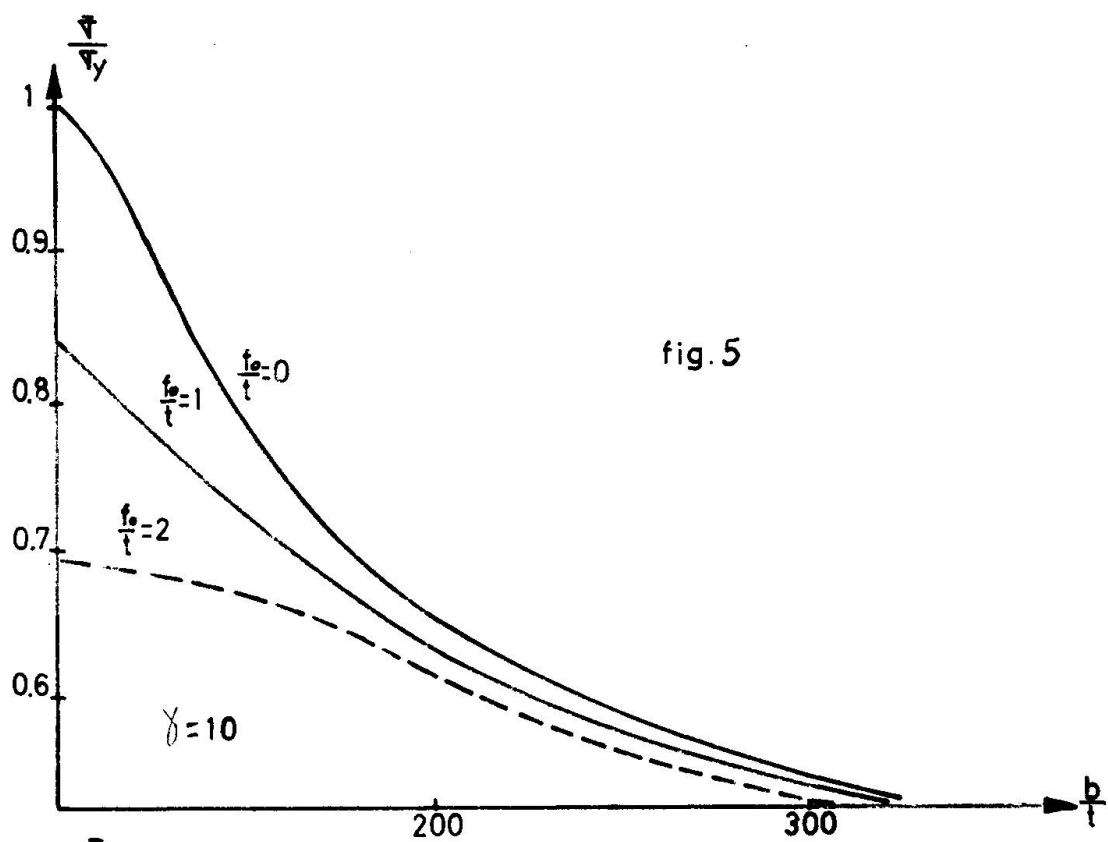
- The two plates have same critical buckling stress according to the linear theory ;
- The ratios of the actual relative rigidity of the stiffeners to the relative optimum rigidity  $\gamma^*$  of the linear theory are identical.

Under these conditions, we assume that the relative reductions of collapse strength are identical for the two plates :

$$\left[ \begin{array}{l} (\bar{\sigma})_{f_o/t=n}^2 \text{ stiff.} \\ (\bar{\sigma})_{f_o/t=0}^2 \text{ stiff.} \end{array} \right] \left( \frac{\gamma_2 \text{ stiff.}}{\gamma_2^* \text{ stiff.}} \right) = m = \left[ \begin{array}{l} (\bar{\sigma})_{f_o/t=n}^1 \text{ stiff.} \\ (\bar{\sigma})_{f_o/t=0}^1 \text{ stiff.} \end{array} \right] \left( \frac{\gamma_1 \text{ stiff.}}{\gamma_1^* \text{ stiff.}} \right) = m \quad (5)$$

$$\sigma_{cr}^2 \text{ stiff.} = K \quad \sigma_{cr}^1 \text{ stiff.} = K$$

This generalization is illustrated by example 2 hereafter.



We shall now try to simulate by numerical examples the conditions existing at collapse in the case of the bridge over the Danube (cf. Section 2) namely an actual stress amounting to the critical stress given by linear buckling theory, because of an error on the actual dead weight distribution and of some additional temperature stresses.

Due to lack of theoretical data, we are obliged however, to consider a square panel in mild steel ( $\sigma_y = 2400 \text{ Kg/cm}^2$ ) stiffened by one or two stiffeners only.

Example N° 1 : box girder bridge with the compressed flange defined by following data :

$\alpha = \frac{a}{b} = 1$ ,  $\gamma = 10$ ;  $\frac{b}{t} = 126$ ; Steel AE24 ( $\sigma_y = 2400 \text{ Kg/cm}^2$ )  
one median longitudinal stiffener.

As the adopted  $\gamma$  is larger than  $\gamma^* = 7$ , the linear buckling theory gives for the buckling coefficient  $k = 4 \times 2^2 = 16$  and the critical stress is

$$\sigma_{cr} = 1920 \text{ Kg/cm}^2.$$

If we follow the Austrian Specifications for erection conditions, we should adopt for design stress the lowest of the two ratios (cf. sec. 2) :

$$\frac{\sigma_{cr}}{1.25} = 1536 \text{ Kg/cm}^2$$

$$\frac{\sigma_y}{1.25} = \frac{2400}{1.25} = 1920 \text{ Kg/cm}^2,$$

that means  $1536 \text{ Kg/cm}^2$ .

However, due to above effects, the actual stress has amounted effectively to

$$\sigma_e = \sigma_{cr} = 1920 \text{ Kg/cm}^2.$$

According to the non linear theory of SKALOUD and NOVOTNY, we find, according to figures 5 and 6 :

For  $\gamma = 10$  and  $\frac{f_o}{t} = 0$  :  $\frac{\sigma}{\sigma_y} = 0.895$ , whence  $\bar{\sigma} = 2148 \text{ Kg/cm}^2$

$\frac{f_o}{t} = 1$  :  $\frac{\sigma}{\sigma_y} = 0.785$ , whence  $\bar{\sigma} = 1884 \text{ Kg/cm}^2$

$\frac{f_o}{t} = 2$  :  $\frac{\sigma}{\sigma_y} = 0.682$ , whence  $\bar{\sigma} = 1637 \text{ Kg/cm}^2$

For  $\gamma = 20$  and  $\frac{f_o}{t} = 0$  :  $\frac{\sigma}{\sigma_y} = 0.895$  whence  $\bar{\sigma} = 2150 \text{ Kg/cm}^2$

$\frac{f_o}{t} = 1$  :  $\frac{\sigma}{\sigma_y} = 0.846$  whence  $\bar{\sigma} = 2030 \text{ Kg/cm}^2$

$\frac{f_o}{t} = 2$  :  $\frac{\sigma}{\sigma_y} = 0.805$  whence  $\bar{\sigma} = 1932 \text{ Kg/cm}^2$

We may now calculate the safety given by the effective stress  $\sigma_e = 1920 \text{ Kg/cm}^2$ . The results are given in following table

Values of the effective safety factor for erection conditions  $s = \frac{\bar{\sigma}}{\sigma_e}$

$f_o/t$	$\gamma/\gamma^*$	1,43	2,86
0		1.118	1.118
1		0.981	1.057
2		0.853	1.006

We see that the effective stress may exceed the mean collapse stress according to SKALOUD - NOVOTNY as soon as the initial imperfection of the plate is of the order of the thickness. If it is recalled in addition that the stiffeners of the Danube bridge gave a ratio  $\gamma/\gamma^*$  approximately equal to one only (cf. sec. 2), above table demonstrates that the considered box girder bridge will collapse during erection for values of the relative imperfection  $f_o/t > 1$ .

Example N° 2 : We apply now the generalization to a plate with two stiffeners proposed in this section and represented by formula (5). We assume once more that the effective stress is equal to the critical stress, e.g.  $1920 \text{ Kg/cm}^2$ .

The plate homologous to that of example 1 has the following characteristics :

$$\gamma_{2 \text{ stiff}} = \gamma_{2 \text{ stiff}}^* \times \frac{\gamma_{1 \text{ stiff}}^*}{\gamma_{1 \text{ stiff}}} = 11.33 \times \frac{10}{7} = 16.2$$

$\gamma_{2 \text{ stiff}}$  being larger than  $\gamma_{2 \text{ stiff}}^*$ , the two stiffeners remain straight according to linear theory and  $k = 4 \times 3^2 = 36$ .

$$\frac{b}{t} = \sqrt{\frac{36 \times 1,900,000}{1920}} = 189$$

From figure 4b, one has

$$\left[ \left( \frac{\bar{\sigma}}{\sigma} \right)_{\gamma}^* f_o/t = 0 \right]_{\gamma = 16,2} = 0.9 \text{ (limit curve)}$$

$$\frac{b}{t} = 189$$

whence

$$(\bar{\sigma})_{f_o/t}^2 \text{ stiff} = 21.60 \text{ Kg/cm}^2$$

and therefore, according to formula (5)

$$\text{for } \frac{f_o}{t} = 1 : (\bar{\sigma})_{f_o/t=1}^2 \text{ stiff} = 21.60 \times \frac{1884}{2148} = 1893 \text{ Kg/cm}^2$$

$$\frac{f_o}{t} = 2 : (\bar{\sigma})_{f_o/t=2}^2 \text{ stiff} = 2160 \times \frac{1637}{2148} = 1643 \text{ Kg/mm}^2.$$

The safeties during erection are therefore respectively :

$f_o/t$	$\gamma/\gamma^*$
	1,43
0	1.125
1	0.986
2	0.855

and the same conclusions as for example 1 ensue.

## 7. EFFECTIVE WIDTH FORMULAE.

It is well known that the irregular stress distribution across the width  $b$  of the plate (fig. 1) with mean value  $\bar{\sigma}$  and maximum value  $\sigma_{\max}$  may be replaced by a uniform distribution of the maximum stress  $\sigma_{\max}$  on a fictitious width called effective width. For equal resultants, we need

$$\sigma_{\max} b_e = \bar{\sigma} b$$

whence

$$\frac{b_e}{b} = \frac{\bar{\sigma}}{\sigma_{\max}} = \phi \quad (6)$$

If the stiffeners remain rigid up to collapse, we admit that the maximum stress  $\sigma_{\max}$  is attained also in the plate at each junction with the stiffeners, so that the effective width formula may be applied to the subpanels.

Let us call :

$\sigma_{cr}$  : the critical stress of buckling of a sub-panel ;

$\sigma_{\max}$  : the maximum membrane stress at the edges of a subpanel, taken equal to  $\sigma_y$  at collapse according to SKALOUD's criterion adopted in section 4;

$\beta$  : the ratio of the width  $b$  of a subpanel by the half wave length of longitudinal buckling.

Among the formulae proposed for the effective width for the considered case (simply supported edges and free relative movement of these edges) we shall retain the following

$$\phi = 0.44 + 0.56 \frac{\sigma_{cr}}{\sigma_{\max}} \quad (\text{PAPCOVITCH}) \quad (7)$$

$$\phi = \sqrt[3]{\frac{\sigma_{cr}}{\sigma_{\max}}} \quad (\text{MARGUERRE}) \quad (8)$$

$$\phi = \sqrt{\frac{\sigma_{cr}}{\sigma_{max}}} \quad (\text{von KARMAN}) \quad (9)$$

$$\phi = \frac{1 + \beta^4}{3 + \beta^4} + \frac{2}{3 + \beta^4} \left( \frac{\sigma_{cr}}{\sigma_{max}} \right) \quad (\text{SECHLER}) \quad (10)$$

$$\phi = \sqrt{\frac{\sigma_{cr}}{\sigma_{max}}} (1 - 0.22 \sqrt{\frac{\sigma_{cr}}{\sigma_{max}}}) \quad (\text{WINTER}) \quad (11)$$

$\frac{\sigma_{cr}}{\sigma_{max}}$  WOLMIR [12] indicates however that formula (8) applies only for  $\frac{\sigma_{cr}}{\sigma_{max}} > 0.2$ . He mentions also that formula (9) of von KARMAN is especially applicable in the case of stiffeners whose relative rigidity is much less than  $\gamma_p^*$ . The same is true for formula (11) of WINTER, which derives from von KARMAN's formula.

The table which follows gives the values of  $\phi = \frac{b_e}{b}$  for various plates, calculated with formulae (7) to (11), and compares them with the values obtained by the theory of SKALOUD-NOVOTNY.

The comparison of the results shows that the results of PAPCOVICH, SECHLER and SKALOUD agree generally sufficiently well. The MARGUERRE values also are satisfactory in the domain  $\frac{\sigma_{cr}}{\sigma} > 0.2$ , whereas the values derived from the KARMAN and WINTER formulae are substantially lower. Using formulae (7) and (10) which are the most satisfactory, we have tested the result obtained experimentally by DUBAS with his test specimen N° 1.

nombre de raidisseurs	Données					PAPCO-VITCH	(*) MARGUERRE	(*) von KARMAN	(*) SECHLER	(*) WINTER	SKALOUD
	$\frac{b}{t}$	$\frac{b'}{t}$	$\alpha'$	$\frac{\sigma_{cr}}{\sigma_{max}}^2$	$\frac{\sigma_{cr}}{\sigma_y}$						
1	200	100	2	759	0.316	0.617	0.680	(0.563)	0.658	(0.493)	0.65
1	270	135	2	417	0.174	0.537	(0.558)	(0.417)	0.587	(0.378)	0.58
1	360	180	2	240	0.100	0.496	(0.464)	(0.316)	0.550	(0.294)	0.54
1	450	225	2	150	0.062	0.475	(0.396)	(0.249)	0.531	(0.235)	0.53
2	210	70	3	1550	0.646	0.802	0.865	0.804	0.823	(0.662)	0.82
2	300	100	3	759	0.316	0.617	0.680	(0.563)	0.658	(0.493)	0.66
2	375	125	3	486	0.202	0.553	0.598	(0.450)	0.601	(0.409)	0.60
2	450	150	3	337	0.140	0.518	(0.520)	(0.374)	0.570	(0.344)	0.57

Values of  $\phi = \frac{b_e}{b}$  or  $\frac{b_e'}{b'}$  for a stiffened plate ( $\alpha = 1$ ) whose stiffeners remain rigid up to collapse, for  $\sigma_{max} = \sigma_y = 2400 \text{ Kg/cm}^2$ .  
 (\*) see the remarks made after formula (11)

## 8. APPLICATION TO DUBAS TEST N° 1

For the actual dimensions of the model DUBAS, the parameters have following values :

thinness of the plate :  $\frac{b}{t} = 242$  ;  
 side ratio of the panel :  $\alpha = 1.125$   
 relative rigidity :  $\gamma = 17.7$   
 relative area :  $\delta = 0.041$

From these characteristics, DUBAS draws from his buckling chart (Fig.4) pertaining to a uniformly compressed plate with three longitudinal stiffeners the value of the buckling coefficient

$$k = 50.7.$$

As the "optimum" relative rigidity  $\gamma^*$ , in the sense of the linear theory, is about 20, the stiffeners will be deformed by the plate and this fact has, indeed, been observed experimentally by DUBAS.

The critical stress calculated by linear buckling theory is

$$\sigma_{cr}^{lin} = 50.7 \cdot \frac{1,900,000}{(\frac{b}{t})^2} = 1640 \text{ Kg/cm}^2.$$

From the measurements made for  $P = 1.75 t$ , a load for which the whole cross section is effective, we calculate the value of coefficient

$$K = \frac{\sigma}{P} = \frac{335}{1750} = 192 \cdot 10^{-3} \text{ cm}^{-2}.$$

As the experimental collapse observed by DUBAS does not coincide with SKALOUD's collapse criterion adopted in present paper (sec. 4), we must assume that collapse occurs when the yield point  $\sigma = 3000 \text{ Kg/cm}^2$  is reached at the edges of the stiffened plate, or, equivalently, when  $\epsilon$  reaches

$\frac{3000}{2,100,000} = 1.43\%$ . From the  $(P, \epsilon)$  diagram given by DUBAS (his fig. 8), we see that corresponding load is  $P = 7.4 t$  and constitutes our collapse load. The corresponding mean compressive stress calculated by NAVIER formula

$$\bar{\sigma}_{exp}^{(1)} = 192 \cdot 10^{-3} \times 7400 = 1420 \text{ Kg/cm}^2$$

is the experimental collapse stress.

This stress is less than the critical buckling stress of the linear theory in the ratio

$$\frac{\bar{\sigma}_{exp}^{(1)}}{\sigma_{cr}^{lin}} = \frac{1420}{1640} = \frac{1}{1.15}.$$

If now be abandon SKALOUD's collapse criterion and revert to the experimental collapse load  $P = 7.95 t$  observed by DUBAS, we have to adopt as collapse stress  $\bar{\sigma}_{exp}^{(2)} = 1525 \text{ Kg/cm}^2$ .

It is seen that this collapse stress of the whole structure is lower than the critical stress of the stiffened plate given by linear theory, which justifies the statement made at the beginning of the introduction of this paper.

In his report, professor DUBAS has applied the effective width formula to estimate the magnification factor  $m = \gamma^*/\gamma^*$  of the stiffeners. By applying effective width formulae (7) and (10) <sup>P</sup>to the full plate of DUBAS considered as unstiffened, we obtain successively :

$$\beta = a = 1.125 ; \sigma_{cr} = \frac{7,593,400}{(242)^2} = 130 \text{ Kg/cm}^2 ; \sigma_{max} = \sigma_y = 3000 \text{ Kg/cm}^2$$

$$\frac{\sigma_{cr}}{\sigma_y} = 0.0434.$$

a) PAPCOVITCH formula (7) gives  $\frac{b_e}{b} = 0.465$  whence  $\bar{\sigma} = 1395 \text{ Kg/cm}^2$ .

b) SECHLER formula (10) gives  $\frac{b_e}{b} = 0.475$  whence  $\bar{\sigma} = 1425 \text{ Kg/cm}^2$ .

We see that a rather good agreement exists between the experimental value  $\bar{\sigma}_{exp}^{(2)} = 1525 \text{ Kg/cm}^2$  and the two theoretical estimates.

However, in principle, the use of an effective width formula for the entire plate is not permissible when this plate is stiffened, because the stiffeners increase the stability of the plate, even if they do not remain straight. One of the main aims of future research is precisely to establish the effect of this kind of stiffeners on the mean collapse stress.

The rather good agreement obtained hereabove between DUBAS test and effective width formulae (7) and (10) only means that the stiffeners of DUBAS first test have a very low efficiency in the collapse stage. The unstiffened plate has a very low buckling stress ( $130 \text{ Kg/cm}^2$ ), but above calculations show that it has a very large postbuckling strength, which is nearly the same as that of the stiffened plate.

## 9. RECOMMENDATIONS FOR FUTURE RESEARCH.

Research on stiffened box girders has to be pushed forward theoretically as well as experimentally.

In the field of theoretical research, we need first calculations of the same type as those developed by SKALOUD and NOVOTNY, but for a larger number of stiffeners.

A second phase would consist to investigate the effect of new parameters, such as geometrical imperfections, welding residual stresses, dissymmetry of the stiffeners with respect to the mean plane of the stiffened plate, effect of the relative area  $\delta$  of the stiffeners and of their eventual torsional rigidity (in the case of closed section stiffeners).

From all these non linear calculations, practical design charts should be built, which would take account realistically of the conflicting effects of imperfections and postcritical resistance.

In parallel with above theoretical studies, an important series of tests should be undertaken to control the theoretical results. In particular, we need some fatigue tests to investigate the effect of the repeated "breathing" of the compressed flange due to its imperfections. In waiting for the conclusions of such researches, the safety factors against buckling should be immediately increased for box girders, so as to avoid new accidents.

## REFERENCES.

- [1] MASSONNET, Ch.: Essais de voilement sur poutres à âme raidie. Mémoires A.I.P.C., Vol. 14, pp. 125 - 186, Zürich 1954.
- [2] MASSONNET, Ch.: Stability considerations in the design of plate girders. Proceedings of the American Institute of Civil Engineers, Journal of Structural Division, Vol. 86, Janvier 1960, pp. 71 - 97.
- [3] OWEN, D.R.J., ROCKEY, K.C., SKALOUD, M.: Ultimate load behaviour of longitudinally reinforced webplates subjected to pure bending. Mém. AIPC, vol. 18, pp. 113-148, Zürich 1970.
- [4] CICIN, P. : Betrachtungen über die Bruchursachen der neuen Wiener Donaubrücke - Tiefbau, Vol. 12, pp. 948 - 950, 1970.
- [5] SATTLER, K. : Betrachtungen über die Bruchursachen der neuen Wiener Donaubrücke - Tiefbau, Vol. 12, pp. 665-674, 1970.
- [6] DUBAS, P. : Essai sur le comportement postcritique de poutres en caisson raidies. Publication préliminaire. Colloque AIPC, Londres, 25 et 26 mars 1971.
- [7] SKALOUD, M. et NOVOTNY, R.: Überkritisches Verhalten einer gleichförmig gedrückten, in der mitte mit einer Längsrippe verstieften Platte. Acta Technica CSAV n° 3, 1964.
- [8] SKALOUD, M. et NOVOTNY, R.: Überkritisches Verhalten einer gleichförmig gedrückten, in der dritteln mit zwei Längsrippen verstieften Platte. Acta Technica CSAV n° 6, 1964.
- [9] SKALOUD, M. et NOVOTNY, R.: Überkritisches Verhalten einer anfänglich gekrümmten gleichförmig gedrückten, in der mittemit einer Längsrippe verstieften Platte. Acta Technica CSAV n° 2 1965.
- [10] SKALOUD, M.: Grundlegende Differentialgleichungen der Stabilität orthotroper Platten mit Eigenspannungen. Acta Technica CSAV n° 4, 1965.
- [11] SKALOUD, M.: Le critère de l'état limite des plaques et des systèmes de plaques. Contribution au Colloque sur le comportement postcritique des plaques utilisées en Construction Métallique, Liège, 12 et 13 novembre 1962.
- [12] WOLMIR, A.S. : Biegsame Platten und Schalen. V.E.B. Verlag für Bauwesen, Berlin, 1962.

Leere Seite  
Blank page  
Page vide

## Ultimate Strength of Plates When Subjected to In-Plane Patch Loading

Résistance à la ruine des âmes soumises à des charges transversales locales

Tragfähigkeit von Stehblechfeldern bei örtlicher Randstreckenlast

**K.C. ROCKEY**  
 M.Sc., Ph.D., C.Eng., F.I.C.E.  
 Professor of Civil  
 and Structural Engineering

University College, Cardiff, England

**M.A. EL-GAALY**  
 M.S.E., D.Sc., M.ASCE.  
 Research Fellow  
 Department of Civil  
 and Structural Engineering

### 1. INTRODUCTION

Frequently web plates are subjected to local in-plane compressive patch loading, such as that shown in figure 1. If the depth to thickness ratio of the web is sufficiently high then it will buckle before it fails. Such web buckling is not synonymous with failure but simply represents a transition from one load carrying mechanism to another load carrying mechanism and the present study has been conducted to obtain relationships between the ultimate load capacity of a panel and its buckling load.

The test program involved a study of how the ultimate load varied with the loading parameter  $\beta$  ( $= c/b$ ), the panel aspect ratio  $\alpha$  ( $= b/d$ ) and the slenderness ratio  $(d/t)$ . It will be shown that a linear relationship exists between the ratio of the ultimate load to the buckling load of a panel and its slenderness ratio  $\frac{d}{t}$  and the loading parameter,  $\beta$ .

### 2. ELASTIC BUCKLING LOADS

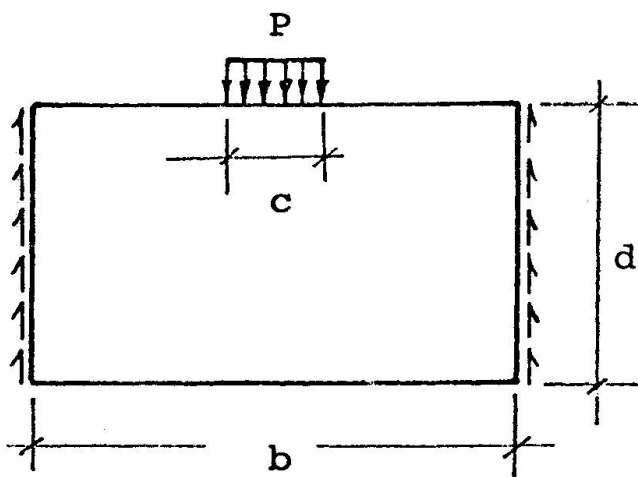


Fig. 1

Theoretical critical load values have been determined for the buckling of plates when subjected to uniform edge load and also for the more difficult case of a panel subjected to partial edge loading (1 - 10). Rockey and Bagchi (10) used the Finite Element Method to determine the buckling load of a rectangular panel when subjected to a patch load on one longitudinal edge and supported by shear forces on the two transverse edges as shown in figure 1. Results were also obtained for the cases where an in-plane moment or an in-plane

shear stress acts in addition to the stress field set up by the patch loading.

The compressive patch load ( $P_{cr}$ ) which will cause buckling of a rectangular plate is given by equation (1).

$$\frac{P_{cr}}{bt} = K \frac{\pi^2 D}{d^2 t} \quad (1)$$

Figure 2, gives the relationship between the non-dimensional buckling coefficient  $K$ , the loading parameter  $\beta$  ( $= c/b$ ) and the aspect ratio  $\alpha$  ( $= b/d$ ).

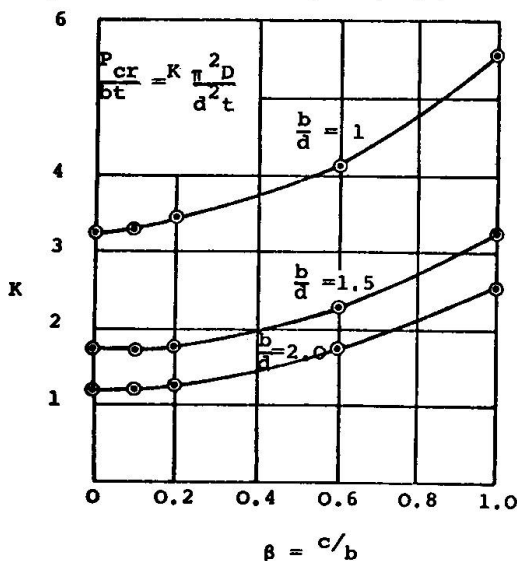


Fig. 2. Variation of the buckling coefficient  $K$  with the loading parameter  $\beta$  and the panel aspect ratio  $b/d$ .

The presence of either an additional shear or moment will reduce the applied edge load necessary to buckle the panel. Figure 3 presents the interaction curves which have been obtained for the following two cases,

(i) a simply supported square plate subject to a combination of uniform edge-loading and in-plane moment

(ii) a simply supported square plate subject to a combination of discrete edge loading ( $\beta = 0.2$ ) and in-plane moment

Figure 4 gives the corresponding interaction curves for the combination of a transverse edge loading and an additional uniform shear load.

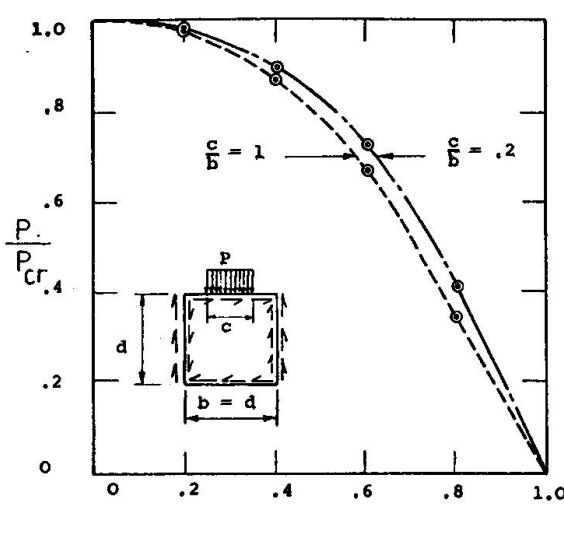


Fig. 3. Influence of a co-existent shear upon the magnitude of the critical patch load.

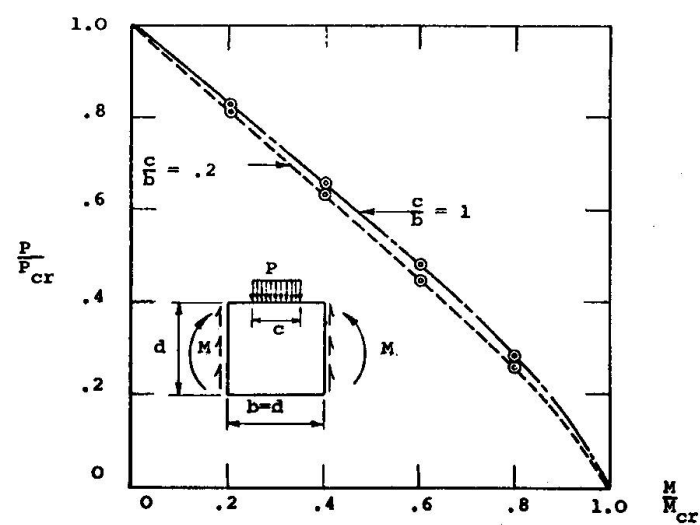


Fig. 4. Influence of a co-existent bending moment upon the magnitude of the critical patch load.

### 3. TEST PROGRAM

The tests were conducted to determine the ultimate load strength characteristics of the webs of a sheet steel flooring system. Figure 5 shows the cross section of the unit (one bay) which was tested.

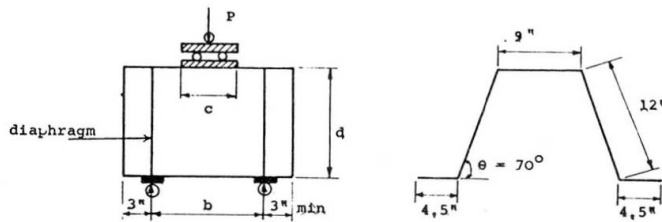


Fig. 5. Details of Test Specimen.

and was distributed over a distance  $c$ , an electric load cell was placed between the ram and the test specimen as can be noted in the figure.

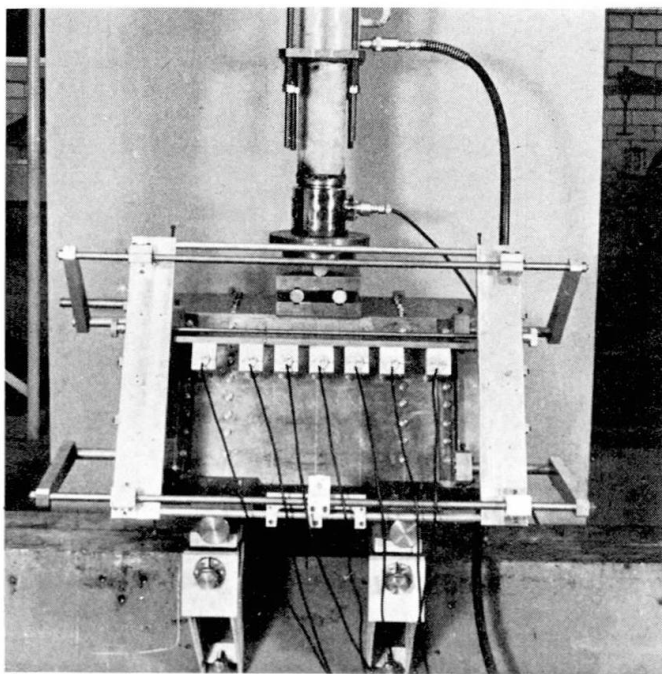


Fig. 6.

any lateral deflection readings were taken.

To determine the material properties three test coupons were tested from each plate to determine the yield stresses and other material properties. All of the test coupons behaved in a manner typical of that expected for mild structural steel and the results showed that the yield stress did not vary markedly from one gauge of material to another.

The test specimen was supported on roller supports which could be adjusted to ensure that the load was applied to both webs. At each support a very strong diaphragm was fitted and straps were fitted across the base of the specimen thus ensuring that no splaying of the webs would occur.

The specimens were tested in a self straining frame and the load was applied by means of a push type hydraulic ram through a central roller  $c$ , as shown in figure 6. An

The lateral deflection of the web was recorded using the special deflection recording apparatus shown in figure 6. With the aid of this frame, the seven linear displacement transducers could be adjusted to any position. These transducers were connected to a data logger which printed out directly the values of the deflections in units of 0.001 inch. In addition, dial gauges, calibrated in units of 0.001 inch were used to record the lateral deflections at specific positions.

Loads were applied to the test specimens in small increments in the elastic range, and in smaller increments after yielding had begun. In the inelastic range, all plastic flow was allowed to take place at each load increment before

## 4. EXPERIMENTAL RESULTS

TABLE 1.

Test No.	d inch	b inch	c inch	t inch	$\alpha = \frac{b}{d}$	$\beta = \frac{c}{b}$	$\frac{d}{t}$	$P_u$ tons	$P_{cr}$ tons	$\frac{P_u}{P_{cr}}$
1.1	12	12	2.4	.037	1	.2	325	.37	.17	2.17
1.2	12	12	2.4	.048	1	.2	250	.54	.38	1.43
1.3	12	12	2.4	.06	1	.2	200	.84	.74	1.13
1.4	12	12	2.4	.075	1	.2	160	1.30	1.43	.91
1.5	12	12	2.4	.102	1	.2	118	2.56	3.58	.72
1.6	12	12	2.4	.128	1	.2	94	4.20	7.08	.59
2.1	12	12	6	.037	1	.5	325	.58	.19	3.06
2.2	12	12	6	.048	1	.5	250	.85	.43	1.98
2.3	12	12	6	.06	1	.5	200	1.23	.83	1.48
2.4	12	12	6	.075	1	.5	160	2.04	1.61	1.27
2.5	12	12	6	.102	1	.5	118	3.95	4.04	.98
2.6	12	12	6	.128	1	.5	94	6.08	7.96	.76
3.1	12	12	1.2	.06	1	.1	200	.71	.70	1.01
3.2	12	12	2.4	.06	1	.2	200	.84	.74	1.13
3.3	12	12	3.6	.06	1	.3	200	.97	.76	1.27
3.4	12	12	4.8	.06	1	.4	200	1.1	.80	1.38
3.5	12	12	6	.06	1	.5	200	1.23	.83	1.48
4.1	12	18	3.6	.037	1.5	.2	325	.41	.13	3.15
4.2	12	18	3.6	.048	1.5	.2	250	.54	.29	1.90
4.3	12	18	3.6	.06	1.5	.2	200	.86	.57	1.51
4.4	12	18	3.6	.102	1.5	.2	118	2.5	2.77	.90
4.5	12	18	3.6	.128	1.5	.2	94	4.10	5.49	.75

The details of the test program are summarized in Table 1. In all the tests, the section was subjected to a patch load together with the reactive shear forces.

Figure 7 shows how the lateral deflection across the central section of the panel varied throughout the test. It will be noted that the deformations are located in the upper half of the panel adjacent to the patch load.

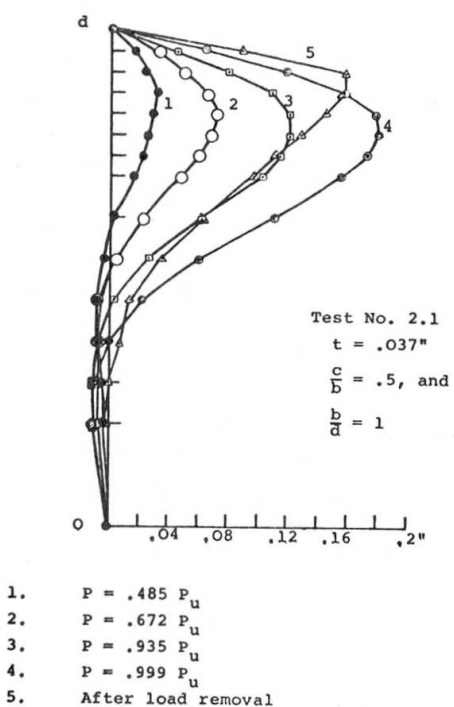


Fig. 7. Variation of lateral deflection of web at the mid section with increasing values of the patch load  $P$ .

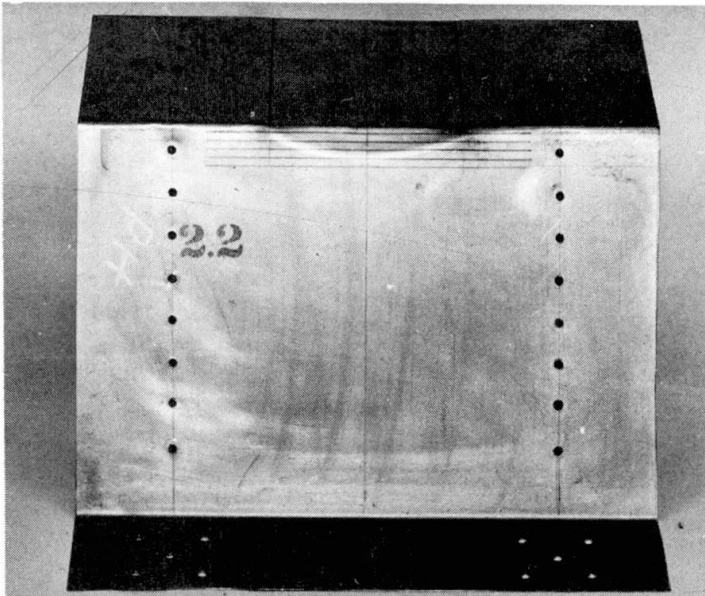
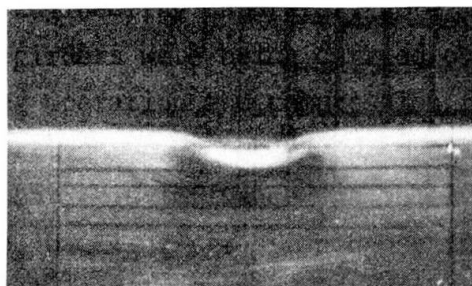
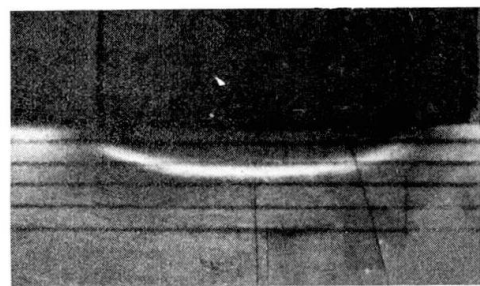


Fig. 8. Failure of a Test Panel showing yield curve.

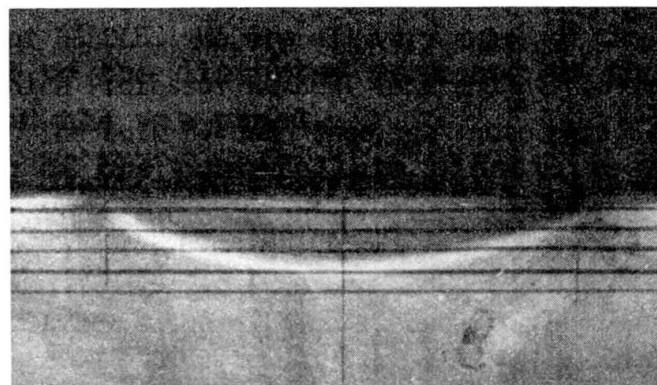
A most significant result is the failure mechanism, in all of the tests failure occurred by the formation of a local yield curve, as shown in figure 8. This yield curve corresponds closely to a segment of a circle, and has a width equal to that of the patch load. It was also noted that the depth of the curve is proportional to the width of the load as can be seen in figure 9. The grid lines in figure 9 are of equal spacing and the variation in the depth of the curve with the  $c/b$  ratio is clearly seen. It was also observed that the shape of the yield curve did not vary with  $d/t$  values.



$c/b = 0.1$  ( $c = 1.2''$ )



$c/b = 0.3$  ( $c = 3.6''$ )



$c/b = 0.5$  ( $c = 6.0''$ )

Fig. 9. Yield Curve Shape and Location on Test Panel ( $b = d$ )

It can be seen, from table 1, that the ratio  $P_u/P_{cr}$  decreases with decreasing values of the  $d/t$  ratio and increases with increasing values of the  $c/b$  ratio. Figure 10 shows how for the specific case of a panel having a depth to thickness ratio of 200:1, the ratio  $P_u/P_{cr}$  varies with the width of the patch load. In figure 11 the  $P_u/P_{cr}$  values for the specific cases of  $c/b = 0.2$  and  $0.5$  and  $\alpha = 1.0$ , are plotted against  $d/t$  values. From figures 10 and 11 the relationship between  $P_u/P_{cr}$ ,  $c/b$  and  $d/t$  given in equation 2 has been obtained.

$$\frac{P_u}{P_{cr}} = \left( 4.5 + 6.4 \left( \frac{c}{b} \right) \right) \frac{d}{t} \times 10^{-3} \quad (2)$$

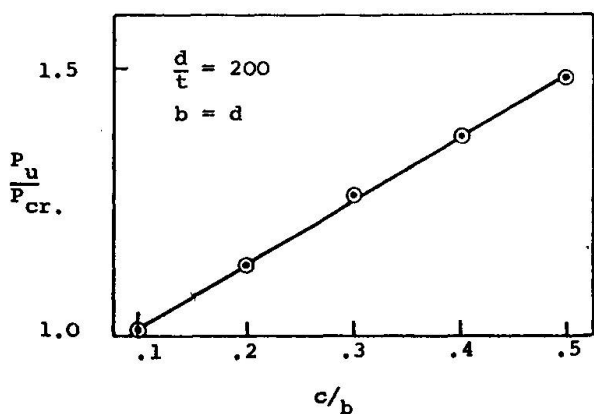


Fig. 10. Variation of the load ratio  $P_u/P_{cr}$  with the load parameter ( $\beta$ ).

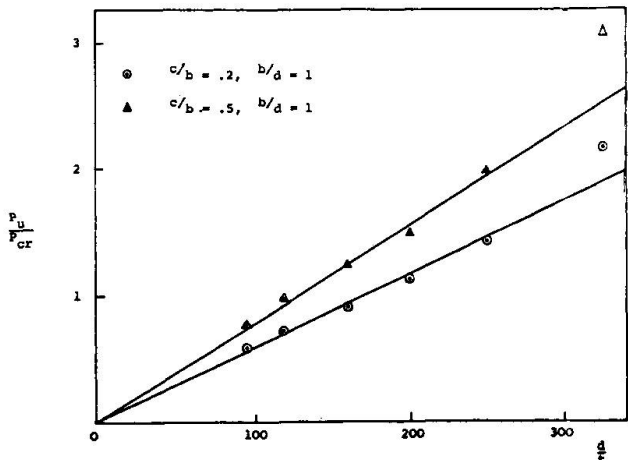


Fig. 11. Variation of the load ratio  $P_u/P_{cr}$  with the slenderness ratio ( $d/t$ ).

Substituting the value of  $c/b = 1.0$  and  $d/t = 288$  into equation 2, it reduces to  $P_u/P_{cr} = 3.14$  which compares closely to the relationship  $P_u/P_{cr} = 3.0$  which Bossert and Ostapenko (11) derived from their tests on panels having a  $d/t$  ratio of 288.

The ratios  $P_u/P_{cr}$  were found to be smaller for the smaller aspect ratio when  $\beta$  is kept constant and equal to 0.2, see table 1. This result contradicts with a conclusion by Bossert and Ostapenko (11) that the post buckling strength varies inversely with the square root of the aspect ratio  $\alpha$ , when  $\beta = 1$  and  $d/t = 288$ . The authors feel that more tests are needed to study the effect of varying  $\alpha$ , and also to examine the influence of flange stiffness upon the ultimate load characteristics. Currently the authors are examining the effect of the presence of an additional shear or moment, see figures 3 and 4, upon the ultimate load characteristics.

## 5. CONCLUSIONS

The test results have shown that there is a considerable amount of post buckling strength for panels having high slenderness ratios. This post buckling strength also increases with the increase in the loading parameter  $\beta$  ( $= \frac{c}{b}$ ). It has been shown that a linear relationship exists between the ratio of the ultimate load ( $P_u$ ) to the buckling load ( $P_{cr}$ ) and the  $c/b$  and  $d/t$  ratios. Failure of all test panels was defined by the formation of a localised yield curve under the load. The width of this curve was found to be equal to that of the load and its depth proportional to its width.

## ACKNOWLEDGEMENT

This study is based on research work conducted for the British Steel Corporation to whom the authors wish to make grateful acknowledgement.

NOTATION

b	length of panel
c	width of patch load
d	depth of panel
D	flexural rigidity of the plate ( $= \frac{Et^3}{12(1-\mu^2)}$ )
d/t	slenderness ratio of panel
E	Young's modulus
K	non-dimensional buckling coefficient
P	applied load
$P_{cr}$	theoretical buckling load
$P_u$	ultimate load
t	thickness of plate
$\alpha$	panel aspect ratio, $\frac{b}{d}$
$\beta$	loading factor, $\frac{c}{b}$
$\mu$	Poisson's ratio

REFERENCES

1. Zommerfield, A.Z., J. Math. Phys. 54 (1906).
2. Timoshenko, S.P., J. Math. Phys. 58, 357 (1910).
3. Girkmann, K., IABSE Final Report (1936).
4. Zetlin, L. Proc. ASCE 81, paper 795 (September, 1955).
5. Wilkesmann, F.W., Stahlbau (October, 1960).
6. White, R.M., and Cottingham, W., J.E.M.Div.Proc. ASCE October (1962).
7. Kloppel, K. and Wagemann, C.H., Stahlbau (July, 1964).
8. Warkenthin, W., Stahlbau (January, 1965).
9. Yoshiki, M., Ando, N., Yamamoto, Y. and Kawai, T., The Society of Naval Architects of Japan, Vol. 12, 1966.
10. Rockey, K.C., and Bagchi, D.K., Int.J.Mech.Sci. Pergamon Press, 1970, Vol. 12, pp. 61 - 76.
11. Bossert, T.W. and Ostapenko, A., Fritz Eng. Lab. Report No. 319.1 (June, 1967).

Leere Seite  
Blank page  
Page vide

### III

#### Additional Study on Static Strength of Hybrid Plate Girders in Bending

Contribution à l'étude de la résistance statique des poutres hybrides fléchies

Zur statischen Tragfähigkeit hybrider Blechträger unter Biegung

YUKIO MAEDA

Dr.-Eng.

Professor of Civil Engineering  
Osaka University, Osaka, Japan

A part of study on ultimate static strength of hybrid plate girders in bending, which is being carried out at Osaka University, is presented in this paper.

#### 1. Static Bending Tests

The concept of "hybrid construction" has been introduced to meet the functional, economic, and safety requirements of a structure. To examine hybrid feature at a plate girder in terms of its static flexural behavior and ultimate strength, four large-scale welded hybrid plate girders with longitudinal stiffeners were tested statically up to their failure under two concentrated loads. Web slenderness ratio of a test panel, which is arranged at the middle part of girder and subjected to a uniform bending moment, was intended for the value of 150, 200, 250 and 300.

A section at the test panel consists of such three steel materials as SM58 for a compression flange, SS41 for a web and HT80 for a tension flange. SM50 steel is used for stiffeners. SS41, SM50 and SM58 steels are specified at the Japanese Industrial Standards, and respectively an ordinary carbon steel, a high-strength structural steel and a high-yield strength quenched and tempered steel. HT80 steel is a high-yield strength quenched and tempered alloy steel, not yet specified at the Japanese Industrial Standards. The average values of upper yield stresses  $\bar{\sigma}_{yu}$ , lower yield stress  $\bar{\sigma}_{yl}$ , tensile strength  $\bar{\sigma}_t$  and elongation  $\varepsilon$  of these steels were shown by coupon tensile tests as follows:

Steel	$\bar{\sigma}_{yu}$ (kg/mm <sup>2</sup> )	$\bar{\sigma}_{yl}$ (kg/mm <sup>2</sup> )	$\bar{\sigma}_t$ (kg/mm <sup>2</sup> )	$\varepsilon$ (%)
HT80	84.64	84.28	88.40	12.3
SM58	54.80	53.64	62.02	19.6
SM50	38.06	36.81	51.52	25.4
SS41	31.44	30.06	42.94	36.5

Sectional areas of the upper and lower flanges of the test girders, are designed so that the both flange materials may reach their yielding stress at the almost same time at the extreme fibers of flanges.

Actual dimensions of the test girders and the yielding stresses of steels for calculations are summarized in Table 1.

#### 2. Discussions of Test Results

(1) Collapse loads  $P_{ex}$ , ultimate bending moments  $M_u$ , modes of failure of test panels and locations of failure are shown in Table 2.

A contribution of web post-buckling strength to ultimate bending strength of the test panel, a benefical effect of longitudinal stiffeners on the web

post-buckling strength and a mode of final failure of the girders being controlled by the rigidity of compression flange and longitudinal stiffeners, have been observed in hybrid girders as well as in non-hybrid girders.

The failure of BL-3 and BL-4 girders is shown in Figs. 1 and 2.

(2) First of all, the web showed a larger lateral deflection after the web yielding at its compression edge for BL-1, -2, and -3 girders and before the web yielding for BL-4 girder, and then the yielding of web penetrated toward the neutral axis of section. Thereafter, the yielding in compression flange developed and extended over its entire thickness, and then its lateral buckling with a torsional buckling in BL-1, -2, and -3 girders and with a vertical buckling in BL-4 girder, was observed. In non-hybrid girders, when a compression flange yielded, a web had not yielded, but in the hybrid girders, the web had already yielded before the flange yielding.

Hence, it follows that the compression flange area alone may resist against a buckling of the flange without a contribution of effective strip of the web, although in non-hybrid girders a compression flange area plus an effective strip of web along the flange can resist flange buckling. At a girder with high hybridness, it will be optimum to select a material for web which buckles at its yielding stress.

Such a behavior can be seen clearly at a typical flexural strain distributions in the test panel of BL-2 and -3 girders as shown in Figs. 3 and 4.

(3) In non-hybrid girders, a loss of web section was observed for a girder with web slenderness ratio larger than 250, but at the present tests the girder with web slenderness ratio of about 300 showed a slight loss of the web section.

(4) Larger initial web deflections were observed for the less rigidities of anchoring frames consisting of flanges and stiffeners. This tendency was recognized more remarkably than in non-hybrid girders. It does not seem that the initial web deflections which were measured to be 0.11 t, 0.36 t, 0.89 t and 1.08 t respectively for BL-1, -2, -3, and -4 girders, influenced greatly on the ultimate strength. The final web deflections were measured to be about 1.0 t - 2.0 t.

(5) Since restraining of the web against a buckling of the compression flange may not be expected after the web yielding, a width-thickness ratio of the compression flange has to be made smaller, to be provided with an equivalent rigidity which is secured by contribution of the effective strip of web section in non-hybrid girders.

(6) The use of a very high strength steel HT80 for the tension flange is beneficial for the compression side of a section, because the neutral axis of the section moves upward, due to the tension flange area about 40% smaller than in non-hybrid girders.

(7) The observed ultimate bending moment  $M_u$  is non-dimensionalized by dividing by the theoretical full-plastic moment  $M_p^{th}$ , as shown in Table 3 and Fig. 5, and  $M_u$  divided by the theoretical flange yielding moment  $M_{yf}^{th}$  is given in Table 3 and Fig. 6. The theoretical moments were calculated following the models of stress and strain in Fig. 7.

The tests of non-hybrid girders consisting of SM58 - SM50 - SM58 showed that the flange yielding moment could be secured up to about  $\beta = h/t_w = 400$ .

At the present hybrid girders of SM58 - SS41 - HT80, however, the possible web slenderness ratio to secure the flange yielding moment has been lowered down to about 300.

Fatigue tests of longitudinally stiffened hybrid plate girders will be soon carried out at Osaka University.

Table 1 Dimensions of Test Girders and Yielding Stresses of Steels

GIRDER	COP.PLANGE ( $2b \times t_c$ mm)	TEN.FLANGE ( $2b \times t_t$ mm)	WEB ( $h \times t_w$ mm)	$t_s \times b_s$ (mm)	$\beta = \frac{h}{t_w}$	$b/t_c$	$\alpha = \frac{a}{b}$	$\gamma/\gamma^*$	$\rho = \frac{A_w}{A_{fc}}$	$\sigma_{yfc}$ (kg/mm <sup>2</sup> )	$\sigma_{yft}$ (kg/mm <sup>2</sup> )	$\sigma_{yw}$ (kg/mm <sup>2</sup> )
BL-1	200×12.9	200×8.0	675×4.8	8×65	141	7.75	1.0	5.34	1.26	53.6	84.3	30.1
BL-2	200×12.9	200×8.0	900×4.8	8×70	188	7.75	1.0	5.67	1.67	53.6	84.3	30.1
BL-3	200×12.9	200×8.0	1125×4.8	8×75	234	7.75	1.0	6.06	2.00	53.6	84.3	30.1
BL-4	200×12.9	200×8.0	1350×4.8	8×80	281	7.75	1.0	6.50	2.50	53.6	84.3	30.1

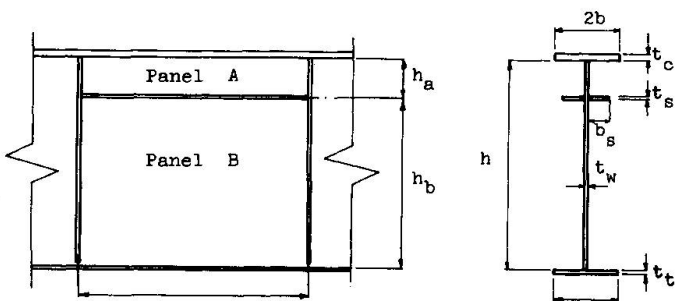


Table 2 Test Results of Failure of Test Girders

GIRDER	$P_{ex}$ (t)	$M_u$ (t-m)	MODE OF FAILURE	LOCATION OF FAILURE
BL-4	147	257	VERTICAL BUCKLING LATERAL BUCKLING	
BL-3	110	220	VERTICAL BUCKLING LATERAL BUCKLING	
BL-2	85	170	OUTSIDE OF TESTPANEL (VERTICAL BUCKLING) LATERAL BUCKLING	
BL-1	62.5	125	OUTSIDE OF TESTPANEL (TORSIONAL BUCKLING) LATERAL BUCKLING	

Table 3 Ultimate Bending Moments

GIRDER	B	$M_u$ (tm)	$M_{yf}^{th}$ (tm)	$M_p^{th}$ (tm)	$M_u / M_{yf}^{th}$	$M_u / M_p^{th}$
BL-1	141	125	111	113	1.126	1.106
BL-2	188	170	156	160	1.090	1.063
BL-3	234	220	205	210	1.073	1.048
BL-4	281	257	259	265	0.992	0.970

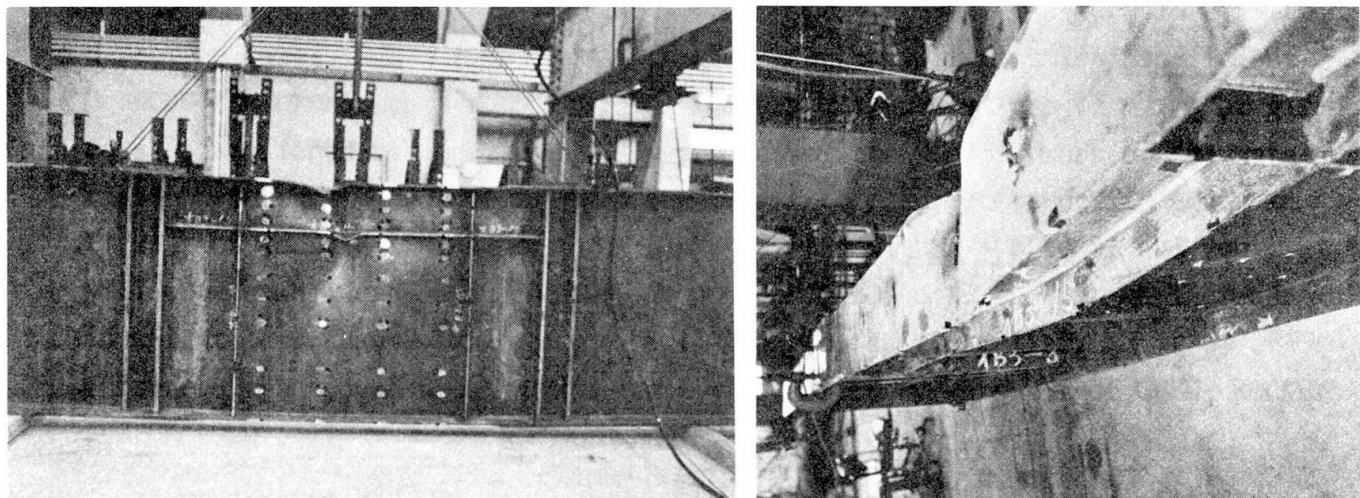


Fig. 1. Failure of Test Girder BL-3

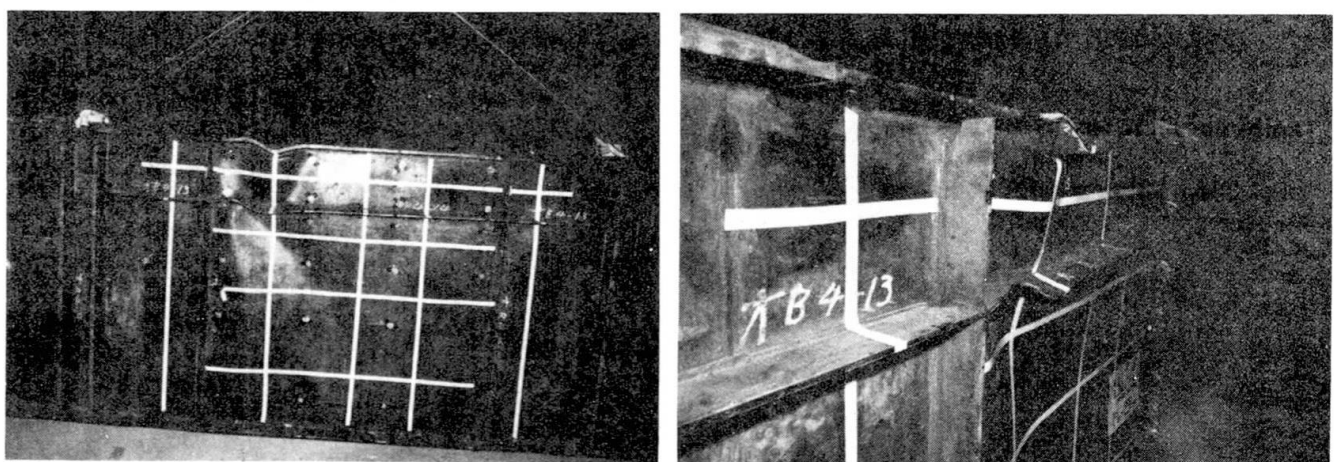


Fig. 2. Failure of Test Girder BL-4

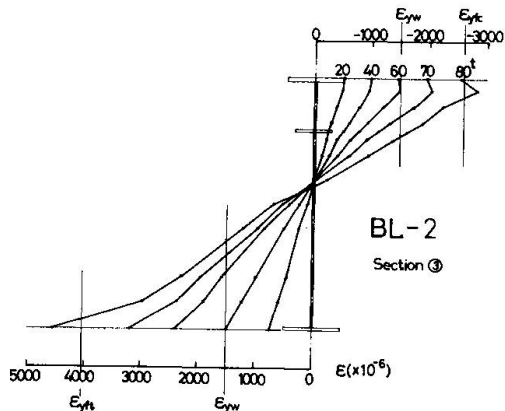


Fig. 3. Strain Distribution in Test Panel of BL-2 Girder

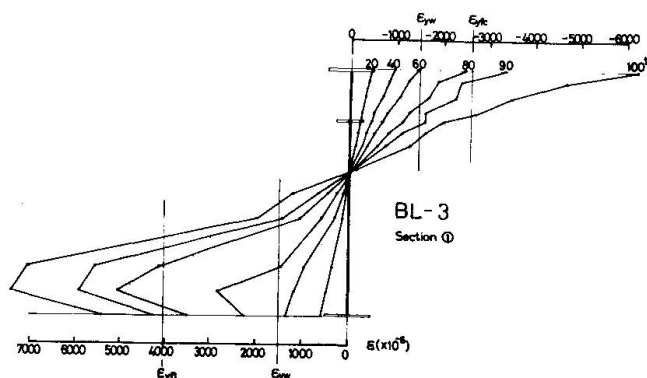


Fig. 4. Strain Distribution in Test Panel of BL-3 Girder

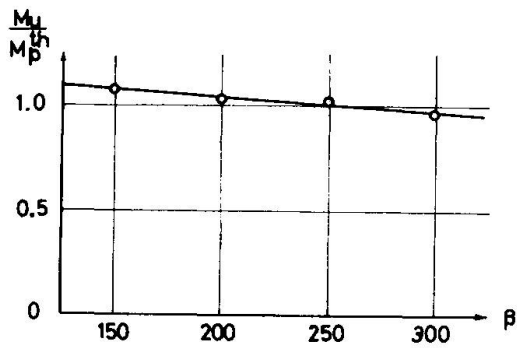


Fig. 5.  $M_u/M_p^{th}$  versus  $\beta = h/t_w$

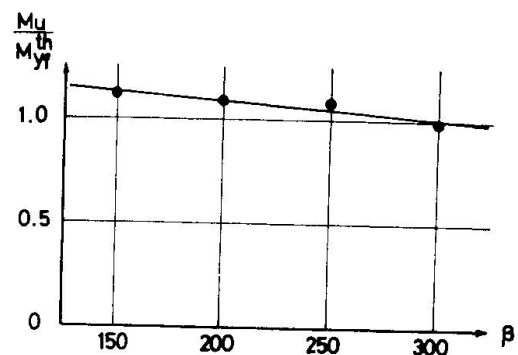


Fig. 6.  $M_u/M_{yf}^{th}$  versus  $\beta = h/t_w$

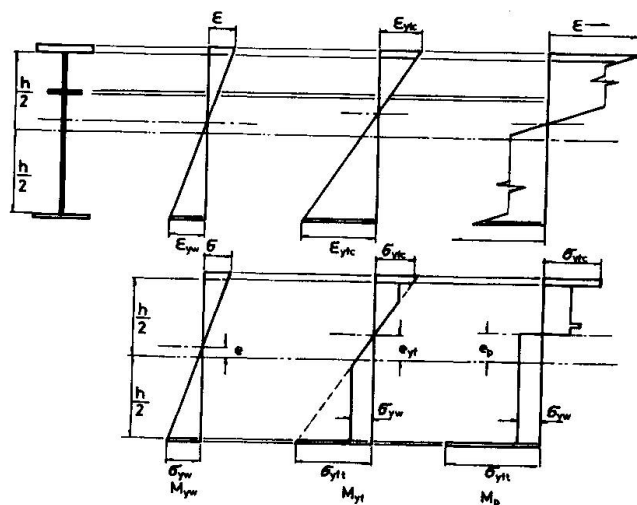


Fig. 7. Models of Development of Stress and Strain

Leere Seite  
Blank page  
Page vide

**Prepared Discussion in regard to the Report Presented by Professor P. Dubas:  
"Essais sur le comportement postcritique de poutres en caisson raidies"**

Discussion préparée du rapport du Prof. P. Dubas:  
"Essais sur le comportement postcritique de poutres en caisson raidies"

Vorbereitete Diskussion zum von Prof. P. Dubas vorgelegten Bericht:  
"Essais sur le comportement postcritique de poutres en caisson raidies"

**MIROSLAV ŠKALOUD**  
Doc., CSc., Ing.  
Senior Research Fellow  
at the Czechoslovak Academy of Sciences  
Institute of Theoretical and  
Applied Mechanics in Prague, Czechoslovakia

The author would like to support the very interesting and valuable conclusions quoted a) in Professor Dubas's report "Essais sur le comportement post-critique de poutres en caisson raidie" and the prepared discussion by Professor Massonnet and R. Maquoi, entitled "The Conventional Design of Box Girders Is Unsafe ....": both regarding the post-buckled behaviour of longitudinally stiffened compression plates of box girders.

Professor Massonnet has already mentioned some of our theoretical conclusions in his prepared discussion. Other theoretical and experimental evidence obtained by our team in Prague has the same trend; therefore, it does not need quoting here.

The author would only like to mention three general conclusions which sum up our main results and observations in the aforesaid field (/1/, /2/, /3/, /4/, /5/):

1) Longitudinal stiffeners designed by the linear theory of web buckling (s.c. concept of  $\beta^*$ ) do not provide sufficient support for the web in the whole post-buckled range of its behaviour. The limit of efficacy of such stiffeners is considerably reduced, so that the stiffeners practically do not operate in a significant part of the post-critical domain of the web in question. The ultimate strength of the plate (and, consequently, the load-carrying capacity of the whole girder) is then

substantially reduced.

2) It was noted that for the longitudinal stiffeners to remain rigid and fully effective up to the collapse of the girder, it was necessary that they should have a flexural rigidity equal to a multiple of the linear theoretical rigidity  $\gamma^*$  ( $\gamma_0 = k \gamma^*$ ).

For such rigid stiffeners, the load-carrying capacity attains the highest possible value. Then the thinnest possible (i.e. optimum) web is obtained.

3) An analysis of our results also indicates that the aforesaid concept is only a limiting case of a more general philosophy.

The relationship between ultimate load and stiffener rigidity is shown in Fig.1. The reader will note there that for small values of  $\gamma$  the ultimate strength grows fast, but then the rate slows down so that, for values near to  $\gamma_0$ , the increase in the load-carrying capacity is only slight.

Therefore, by considerably reducing the stiffener rigidity with respect to  $\gamma_0$ , a very small reduction in ultimate load is obtained. In other words, if the stiffener dimensions are significantly diminished, only a slight increase in web thickness is needed. Considering that the number of available thin sheets of different thicknesses is limited, the slight reduction in load-carrying capacity does not frequently lead to any practical increase in web thickness.

From this it follows that the concept of rigid stiffeners, furnishing an optimum web, need not necessarily lead to the most economic alternative, if the designer has not in mind merely the web (or compression plate element) alone, but desires to optimize

the whole system of web (or plate element) + stiffeners; or, in other words, desires to optimize the whole girder.

To conclude the author wishes to state that he shares the view, quoted in the two afore-mentioned contributions, that the current design concept based on the  $\gamma^*$  - value ought to be abandoned. Further research in regard to the post-buckled behaviour of compression plates fitted with longitudinal stiffeners should be conducted as soon as possible, in order that the aforesaid efficiency factor  $k$  could be determined for various kinds of stiffening. A new design procedure, taking account of the post-critical performance of compressed stiffened elements of

box girders, can then be established; and further accidents, like those of Vienna, Milford Haven and Melbourne, will thereby be avoided.

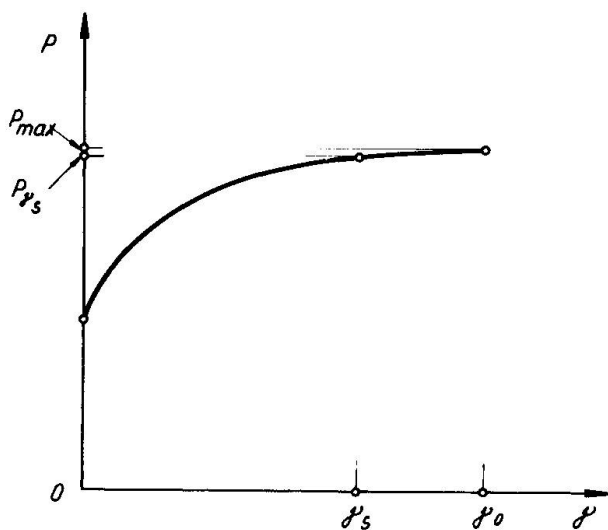


Fig. 1.

References:

- /1/ Škaloud, M., Novotny, R.: Überkritisches Verhalten einer gleichförmig gedrückten, in der Mitte mit einer Längsrippe verstieften Platte. *Acta technica ČSAV*, n° 3, 1964.
- /2/ Škaloud, M., Novotný, R.: Überkritisches Verhalten einer gleichförmig gedrückten, in den Dritteln mit zwei Längsrippen verstieften Platte. *Acta technica ČSAV*, n° 6, 1964.

/3/ Škaloud, M., Novotný, R.: Überkritisches Verhalten einer anfänglich gekrümmten, gleichförmig gedrückten, in der Mitte mit einer Längsrippe verstieften Platte.  
Acta technica, n° 2, 1965.

/4/ Škaloud, M.: Überkritisches Verhalten gedrückter mit nachgiebigen Rippen verstieifter Platten (Experimentelle Untersuchung).  
Acta technica ČSAV, n° 5, 1963.

/5/ Škaloud, M.: Post-buckled behaviour of stiffened webs, Book. Rozpravy ČSAV. Publishing House "Academia", 1970.

**Prepared Discussion in regard to the Post-Buckled Behaviour and  
Incremental Collapse of Webs Subjected to Concentrated Loads**

Discussion préparée du thème:

"The Post-Buckled Behaviour and Incremental Collapse of Webs Subjected  
to Concentrated Loads"

Vorbereitete Diskussion zum Thema:

"The Post-Buckled Behaviour and Incremental Collapse of Webs Subjected  
to Concentrated Loads"

**MIROSLAV ŠKALOUD**

Doc., CSc., Ing.

Senior Research Fellow

at the Czechoslovak Academy of Sciences  
Institute of Theoretical and  
Applied Mechanics in Prague, Czechoslovakia

**PAVEL NOVÁK**

Doc., CSc., Ing.

Research Fellow at the Structural Institute  
in Prague, Czechoslovakia

**Introductory Remarks**

The investigation /1/, /2/ into the post-buckled behaviour of webs in shear having been completed, a new research project regarding the ultimate load behaviour of plate girders was started in Prague. This deals with the effect of flange stiffness upon the ultimate load performance of thin webs subjected to a) static and b) variable repeated concentrated loads, which are applied to the flange of the girder at the mid-distance of the vertical stiffeners of the web. This problem is frequently encountered in the design of crane girders, certain types of bridge girders and similar structures, and also in the case of girders without vertical stiffeners (see the very interesting contribution by Bergfelt /3/). The objective of our new research is to study not only the static failure mechanism of such girders, but also the deflection stability of the web under variable repeated, cyclic loading, and the incremental collapse of the web and the whole girder.

**Test Girders and Apparatus**

The aforesaid research project consists, in the first stage, of testing 8 steel panels shown in Fig. 1 and 7 large-scale steel test girders. Further test series will follow. Some of the panels and girders are subjected to static loads, the others to cyclic pattern loading.

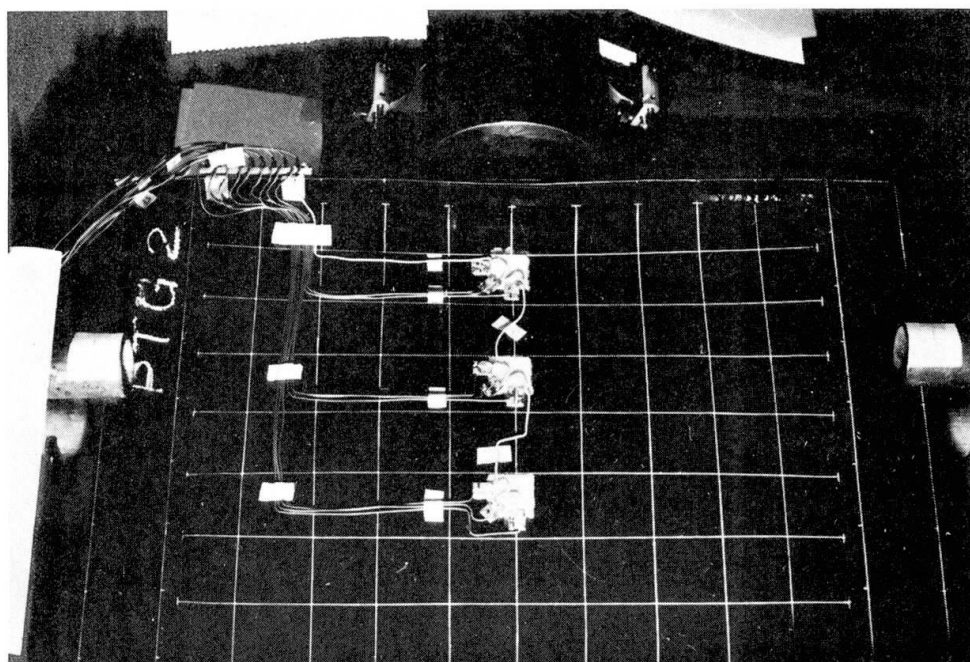


Fig. 1.

The research on steel girders is accompanied by a photo-elasticity investigation conducted by the first of the authors and J. Kratěna on reduced-scale epoxy-resin models.

The buckled pattern of the web is measured by means of a stereophotogrammetric method which has been established by one of the authors /4/. One of the advantages of this method consists in making it possible to measure not only the web deflection perpendicular to the web, but also the other two components of the spatial displacement vector of any point of the web and flanges. Thus it is possible, for instance, to evaluate the distortion, in terms of load, of the projection of the mesh that was marked on the web, and which serves as a basis for the determination of the contour maps of the buckled surfaces of the web. The distortion of the projected mesh is not negligible, as can be seen in an enlarged scale in Fig. 2, this being particularly the case in the vicinity of the applied load. The contour plots of the buckled surface of the

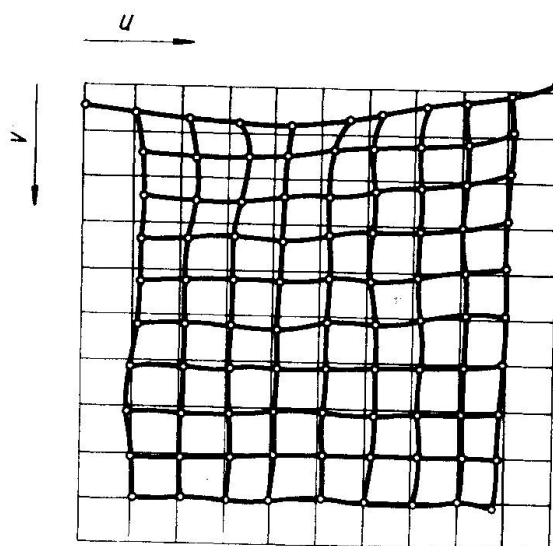


Fig. 2.

web are then related to the distorted mesh and to the deformed boundary framework of the web panel.

The contour map of the post-failure plastic residue in a web panel, subjected to a concentrated load at the mid-distance of the vertical stiffeners, and in the deflected flange are shown in Fig. 3.

The stereophotogrammetric method is also successfully used to measure the web buckled pattern and the flange deflection in the cyclic loading tests. An oscilloscope "Disa" and additional apparatus (Fig. 4) enable the writers to measure the deformation at any time moment of a loading cycle – for instance, at the moment when the deflection amplitude is reached.

The stress state in the web and flanges is measured by numerous electric resistance strain gauges. In the case of cyclic loading, some of the strain gauges and dynamic deflection pick-ups are linked to an automatic recorder "Ultralette", which records

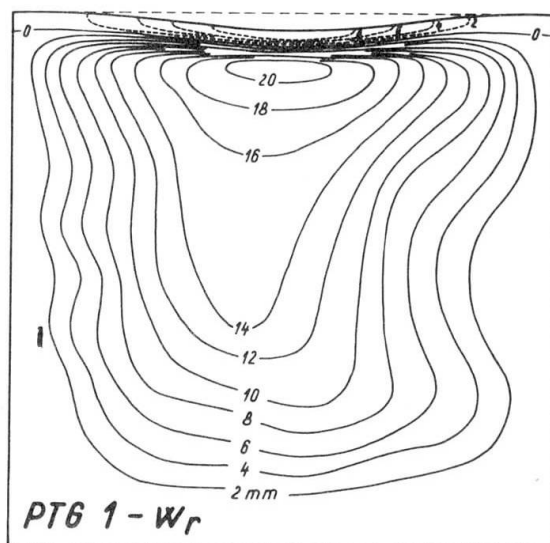


Fig. 3.

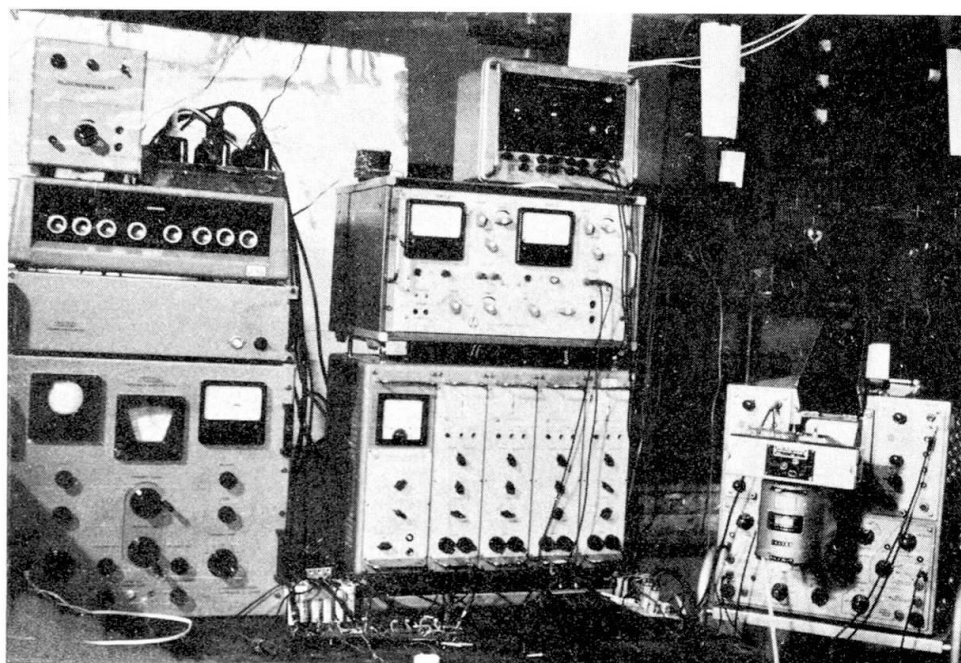


Fig. 4.

the corresponding signals on recording paper (see Fig. 5, showing an increase in web deflection during cyclic loading).

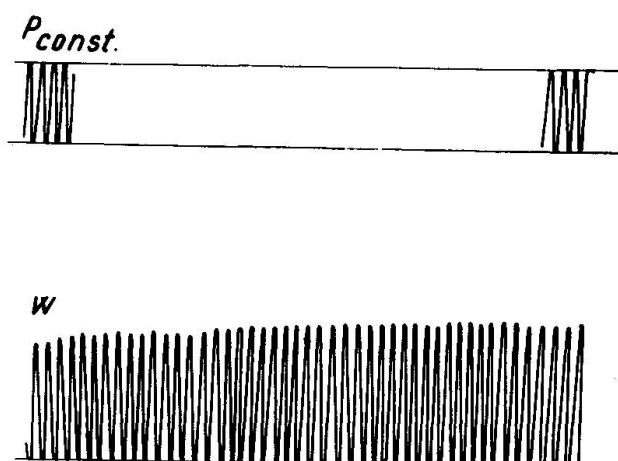


Fig. 5.

Test Results

An analysis of the static test results indicates that thin webs subjected to concentrated loads manifest a considerable post-critical reserve of strength, which ought to be taken into account in the design of steel plate girders.

The load-carrying capacity of such webs is significantly affected by the flexural rigidity of flanges. While for web panels attached to flexible flanges, whose  $I_f/a^3t = 3.49$  ( $I_f/a^3t$  denoting the same flange stiffness parameter as was used in /1/, /2/), the ratio ultimate load  $P_{ult}/$ critical load  $P_{cr} = 1.73$ : in the case of webs attached to heavier flanges,  $I_f/a^3t = 63.5$ , the same ratio amounted, on a average, to 2.445.

In the tests on plate girders subjected to variable repeated loading, the question of stability of post-critical web deflection is of importance.

When the girder operates in the plastic range, an increase in web deflection during a certain number of loading cycles is noted (Fig. 5). The problem is then to determine the maximum load for which these deflection increments cease after a limited number of cycles of load application, and the structure then responds to the load in a purely elastic manner. The corresponding load, which is referred to as the "stabilizing load", is the highest force the girder can sustain. Any further increment in load brings about a breakdown of the girder through incremental collapse.

Fig. 5 relates to a load which was practically equal to the "shake-down load" of the test girder. A slight further increment in load caused instability of web deflection and, shortly afterwards, a collapse of the girder.

A complete report on the above mentioned research project will appear shortly after the completion of the tests.

References:

- /1/ Rockey, K.C., Škaloud, M.: The ultimate load behaviour of plate girders loaded in shear. Contribution presented at the IABSE Colloquium "Design of Plate and Box Girders for Ultimate Strength", London, March, 1971.
- /2/ Škaloud, M.: Ultimate load and failure mechanism of thin webs in shear, dtto.
- /3/ Bergfelt, A.: Studies and tests on slender plate girders without stiffeners. dtto.
- /4/ Novák, P.: Méthode photostéréométrique dynamique des modèles. Colloque International de RILEM, Bucuresti, 9.-11.sept. 1969.

### III

**English Translation of part of the text of pages 13, 14 and 15 of the book:  
Beulwerte ausgesteifter Rechteckplatten, Vol. II by K. Klöppel and  
K.H. Möller, Editor W. Ernst und Sohn, Berlin, 1968  
(Reproduced with the Permission of Professor K. Klöppel)**

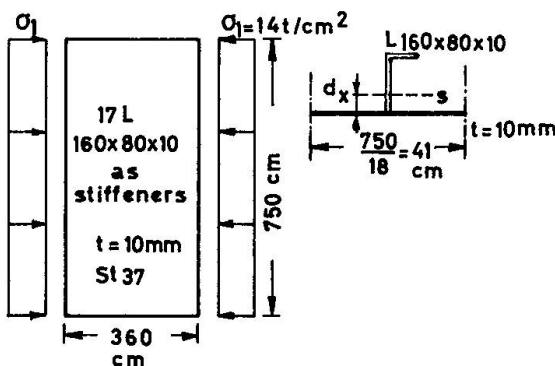
Traduction anglaise d'une part du texte des pages 13, 14 et 15 du livre:  
Beulwerte ausgesteifter Rechteckplatten, Vol. II par K. Klöppel et  
K.H. Möller, Editeur W. Ernst und Sohn, Berlin 1968  
(reproduit avec l'autorisation du Prof. K. Klöppel)

Englische Übersetzung eines Teils des Textes der Seiten 13, 14 und 15 des  
Buches:  
Beulwerte ausgesteifter Rechteckplatten, Bd. II von K. Klöppel und  
K.H. Möller, Verlag W. Ernst und Sohn, Berlin 1968  
(Mit Genehmigung von Prof. K. Klöppel)

#### Page 13.

In the use of tables for uniformly distributed stiffening, it is necessary exert cautiousness about two questions :  
First, about the calculations of the effective moment of inertia,  
secondly, about the safety required against buckling.  
The Standard DIN 4114 Ri 18.13. accepts, for eccentric stiffeners, to relate the moment of inertia to the upper edge of the plate. The basis of this rule is an assumption about the effective width of a corresponding strip of the buckled plate. But when the stiffeners are regularly spaced, the effective width cannot be larger than the distance between two stiffeners.  
If the moment of inertia of such a plate strip is calculated, then values significantly smaller than according to DIN 4114 are usually obtained.  
For closely spaced stiffeners, it is therefore always recommended to calculate the moment of inertia both according to the Standard and also for a plate strip composed of a stiffener and a web strip having as width the distance between two stiffeners, the example figure 11 should serve an illustration. According to DIN 4114, the moment of inertia with respect to the upper edge of the web is

$$J_{\text{DIN}} = J_L + F_L (a - e_x)^2 = 6 \cdot 11 + 23,2 \times (16 - 5,63)^2 = 3115 \text{ cm}^4$$



With the largest value for the effective width, namely the distance between two stiffeners, the distance of the centroid to the upper edge of the web is found to be, according to fig. 11 :

$$d_x = \frac{F_L \left( a + \frac{t}{2} - e_x \right)}{F_L + F_{\text{web}}} = \frac{23,2 \left( 16 + 0,5 - 5,63 \right)}{23,2 + 41} = 3,92$$

which yields

$$J = J_2 = F_L \left( a + \frac{t}{2} - e_x - d_x \right)^2 + F_{\text{web}} \quad d^2 = 2360 \text{ cm}^4$$

It is seen therefore that  $J_{\text{DIN}}$  does not apply for the calculation of the buckling stress.

#### Page 14.

As already mentioned in the Introduction, one has to distinguish between the linear buckling, connected with idealized structural and geometrical assumptions, with the buckling load as limit load, which is the basis for the specification DIN 4114 and for the present book, and a second postcritical non linear buckling, described by non linear differential equations to which is associated a limit load which is called ultimate load. This load is regularly higher than the buckling load, because additional membrane stresses come into play. On this theoretically more complicated way, the influences of unavoidable initial deflections may also, for example, be taken in consideration. The ultimate load above the buckling load can be determined either by the entry into the plastic range or by inacceptably large deformations.

#### Page 15.

It is necessary to come back to the question whether by plate buckling a second equilibrium state establishes itself or not. Let us imagine the plate to be studied by linear buckling theory in the buckled state. In addition to the membrane stresses existing already before buckling, we have now flexural stresses, that may be considered to be produced by the fictitious transverse load

$$q = \sigma_x t \frac{\sigma_w^2}{2} + \sigma_y t \frac{\sigma_w^2}{2} + \tau t \frac{\sigma_x \sigma_y}{2}$$

where  $\sigma_x$ ,  $\sigma_y$  and  $\tau$  are the edge stresses of the plate. If the buckling shape is not known, one shall imagine that the plate is subjected to a uniform transverse load. A large limit load is then to await, when these fictitious transverse loads are supported in all directions nearly on the same way, in other words when we have an extended plate action. If, on the contrary, these imagined transverse loads are supported only in the direction of the greatest compressive stresses, then we can as a good approximation to reality imagine the plate to be cut in strips by cuts parallel to the largest compressive stresses. The individual beamlike strip will then behave like a buckled stilt.

It is recommended now, for plates which support the fictitious transverse loads nearly uniquely in the direction of the large compressive stresses, to require larger safeties than  $\gamma_b = 1,25$  or  $\gamma_h = 1,35$ .

According to the opinion of the authers, which is supported by sections 17.5 and 17.6 of the DIN 4114, safeties are to be required which in the limit case coincide with those for the compressed bar. Numerical comparisons have led to following formule – which cannot be demonstrated, which should give the required safety

$$\frac{\varphi_k}{\varphi_B} = \frac{\varphi_k + 100 \bar{\alpha}^2 \varphi_B}{1 + 100 \bar{\alpha}^2}$$

The side ratio  $\bar{\alpha}$  is obtained through the differential equation of the orthotropic plate, under the assumption of a definite torsional rigidity, by a coordinate transformation.  $\bar{\alpha}$  is the side ratio of an unstiffened comparison plate with the same buckling shape as the stiffened plate :

$$\bar{\alpha} = \alpha \sqrt{\frac{4}{1 + \sum \frac{1}{\lambda_i^2}}}$$

An unstiffened plate with the side ratio  $\alpha$  behave therefore similarly as an unstiffened plate with the side ratio  $\bar{\alpha}$ .

For the above example, (fig.11),  $\lambda_L = 615$  and

$$\bar{\alpha} = 0,48 \sqrt{\frac{4}{615}} = 0,096$$

According to Table 7 of DIN 4114, we have for loading case 1

$$\varphi_k = 2,18$$

and one obtains

$$\frac{\varphi_k}{\varphi_B} = \frac{\varphi_k + 100 \bar{\alpha}^2 \varphi_B}{1 + 100 \bar{\alpha}^2} = 1,69$$

This safety against buckling at least should be required, in this example, in the opinion of the Authers.

In the choice of the stiffener section, it must be in addition taken care that stiffeners do not buckle before reaching the plate buckling load.

Leere Seite  
Blank page  
Page vide

### III

#### **Excerpts of a Letter of Professor F. Leonhardt to Professor Ch. Massonnet (Reproduced with the Permission of Professor F. Leonhardt)**

Extraits d'une lettre du Prof. F. Leonhardt au Prof. Ch. Massonnet  
(reproduits avec la permission du Prof. F. Leonhardt)

Auszüge aus einem Brief von Prof. F. Leonhardt an Prof. Ch. Massonnet  
(abgedruckt mit Bewilligung von Prof. F. Leonhardt)

For the stiffened bottom plate or the bottom flange of a box-girder under negative moments, with compression in the bottom flange, there is almost no post buckling carrying capacity, as the example of the Danube-Bridge demonstrated. After buckling of the bottom flange, the box can usually carry only more or less as a hinge in the elevation of the stronger orthotropic top plate. This situation makes it necessary to calculate the bottom flange more or less like a compressed column with a buckling length equal to the distance of the transverse stiffeners, if the stiffeners have sufficient rigidity. With soft stiffeners the buckling length becomes even larger. Also in this case, we assume a certain eccentricity of the compressive force to take care of unavoidable deviations from the straight line of the axes of the cross-section of a flange (plate plus longitudinal stiffeners). For the longitudinal stiffeners we usually take profiles with a top flange.

The deviations of the actual profiles from the straight lines, which we assume in our calculations, must be laid down on the working drawings and specifications as allowable tolerances and immediately after the erection of portions of the box girder, the actual deviations must be checked and must be kept within these limits.

For the bottom flanges we must also keep in mind, that the principal compressive stresses in the plate are not parallel to the longitudinal axis of the box-girder, but inclined and the angle of inclination depends upon the shear force and the torsion. This can have some influence on the spacing of longitudinal stiffeners and on the buckling safety of the bottom plate itself.

Dimensioning the bottom flange in this way does usually result in only a very small amount of additional steel quantity, because the increased stiffness of the longitudinal stiffeners allows to use a thinner plate. Only the additional rigidity of the transverse stiffeners may increase the weight.

But also here the difference is so small, that it should not count economically.

I am sending to you a drawing of a cross-section of Moseltal-Brücke Winningen, which we have designed along these lines about 2 years ago and which is under construction just now. It has spans up to 240 m and is erected by the free-cantileveringmethod, giving rather high compressive force to the bottom slab.

Leere Seite  
Blank page  
Page vide